INVESTIGATING THE ANNUAL AND SEMI-ANNUAL VARIATIONS OF GEOMAGNETIC FIELD COMPONENTS IN THE NORTHERN HEMISPHERE

BY

ODUBIYI, AYOBAMI A.

PG/M.Sc./10/52401

DEPARTMENT OF PHYSICS AND ASTRONOMY,
UNIVERSITY OF NIGERIA, NSUKKA

SUPERVISOR: PROF. (MRS.) F.N. OKEKE (FAS)

SEPTEMBER, 2014

A PROJECT SUBMITTED TO THE DEPARTMENT OF PHYSICS AND ASTRONOMY, FACULTY OF PHYSICAL SCIENCES, UNIVERSITY OF NIGERIA, NSUKKA IN PARTIAL FULFILMENT OF THE AWARD OF MASTER OF SCIENCE (M.Sc) DEGREE

BY

ODUBIYI, AYOBAMI A.

PG/M.Sc./10/52401

TOPIC

INVESTIGATING THE ANNUAL AND SEMI-ANNUAL VARIATIONS OF GEOMAGNETIC FIELD COMPONENTS IN THE NORTHERN HEMISPHERE

SUPERVISOR: PROF. (MRS.) F.N. OKEKE (FAS)

SEPTEMBER, 2014

CERTIFICATION

This is to certify that the work embodied in this project is original and has not been used in full or partial thereof for any other degree or professional qualification in this or any other university.

_____

ODUBIYI AYOBAMI ADEJUMO

DEDICATION

This project is dedicated to God Almighty and to My Late Mum Mrs. A. O. Odubiyi, May her Soul Continue to rest in the Bosom of the Lord.

ACKNOWLEDGEMENT

First and foremost, I give gratitude to the Almighty, the only Power that exists and who in turn permitted every other thing to come into existence. To Him be all honour and glory for all eternity.

I wish to express my sincere gratitude to my supervisor Prof. (Mrs.) F. N. Okeke for the motherly role she played in guiding me throughout this project work. I will like to thank all the lecturers and my classmates in the Department of Physics and Astronomy University of Nigeria Nsukka. I will also like to acknowledge the adequate support of my colleagues and friends who worked with me on this Project. I appreciate the efforts of my mentor Dr. K. C. Okpala for his relentless positive criticisms that helped me to complete this project successfully.

My gratitude also goes to my parents Mr. S. K. Odubiyi and Late Mrs. A. O. Odubiyi, for being my parent and guardian in its total and truest sense. I appreciate the support of the entire staff of the ICT Unit, University of Nigeria Nsukka. Finally I acknowledge the support and efforts of my brothers; Mr. Adeniran Odubiyi and Mr. Adefemi Odubiyi, my boss; Engr. Sikiru Salawu, and my friends who stood solidly with me through it all.

Thank you all.

Abstract

A study of the ever present ring current on the geomagnetic field strength is used to determine the annual and semi-annual geomagnetic activity variation and validate Russell-McPherron hypothesis. The D, H and Z geomagnetic field component mean monthly and yearly field strength in ten (10) geomagnetic observatories at different geomagnetic longitude were employed. Six parameters representing annual (D_{diff}, H_{diff} and Z_{diff}) and monthly (d_{diff}, h_{diff} and z_{diff}) residuals of the geomagnetic field strength were defined, and presented as indicators of ring current monthly/yearly influence on the strength of the components of the geomagnetic field. It is found that only mid latitude stations showed common pattern of D_{diff} with peaks during solar maximum and troughs during solar minimum, a pattern which follows the SS cycle although out of phase. H_{diff} showed annual variation corresponding to the 11year solar cycle especially in low and mid geomagnetic latitudes which was not in phase with the sunspot number (SSN). The Z_{diff} parameter exhibited annual variation which corresponded also with the 11 year solar cycle in the mid and high latitudes. We observed strong correlation (at 95% confidence) of D_{diff} with SSN for only mid latitude stations. Strong inverse correlation between H_{diff} and SSN was found at low and mid -geomagnetic latitudes and weaker correlation at high latitudes. Statistical association between Z_{diff} and SSN was stronger at high geomagnetic latitudes than low geomagnetic latitudes. The semiannual variation of the parameters- d_{diff}, h_{diff} revealed clear equinoctial peaks in April and Oct-Nov. The fall peak is slightly larger than the spring peak and this observation were the same irrespective of location. This semiannual global seasonal phenomenon is likely dominated by the North-South migration of the ring current

LIST OF TABLES

LIST OF FIGURES

TABLE OF CONTENTS

CHAPTER ONE
INTRODUCTION

1.1 Earth's Atmosphere

The Earth's atmosphere is a layer of gases surrounding the planet Earth that is retained by Earth's gravity. The atmosphere protects life on Earth by absorbing ultraviolet solar radiation, warming the surface through heat retention (greenhouse effect), and reducing temperature extremes between day and night (the diurnal temperature variation).

Atmospheric stratification describes the structure of the atmosphere, dividing it into distinct layers, each with specific characteristics such as temperature or composition. The atmosphere has a mass of about 5×10^{18} kg, three quarters of which is within about 11 km (6.8 mi; 36,000 ft) of the surface. The atmosphere becomes thinner and thinner with increasing altitude, with no definite boundary between the atmosphere and outer space.

Dry air contains roughly (by volume) 78.09% nitrogen, 20.95% oxygen, 0.93% argon, 0.039% carbon dioxide, and small amounts of other gases. Air also contains a variable amount of water vapor, on average around 1%. While air content and atmospheric pressure vary at different layers, air suitable for the survival of terrestrial plants and terrestrial animals is currently only known to be found in Earth's troposphere and artificial atmospheres.

1.1.1 Troposphere

The troposphere is the lowest portion of Earth's atmosphere. It contains approximately 80% of the atmosphere's mass and 99% of its water vapor and aerosols (McGraw-Hill, 1984).

The average depth of the troposphere is approximately 17 km (11 mi) in the middle latitudes. It is deeper in the tropics, up to 20 km (12 mi), and shallower near the Polar Regions, at 7 km (4.3 mi) in summer and indistinct in winter. The troposphere is mostly heated by transfer of energy from the surface, so on average the lowest part of the troposphere is warmest and temperature decreases with altitude. The lowest part of the troposphere, where friction with the Earth's surface influences air flow, is the planetary boundary layer. This layer is typically a few

hundred meters to 2 km (1.2 mi) deep depending on the landform and time of day. The border between the troposphere and stratosphere is called the tropopause

1.1.2 Stratosphere

The stratosphere is the second major layer of Earth's atmosphere, just above the troposphere, and below the mesosphere. It is stratified in temperature, with warmer layers higher up and cooler layers farther down. This is in contrast to the troposphere near the Earth's surface, which is cooler higher up and warmer farther down. The border of the troposphere and stratosphere, the tropopause, is marked by where this inversion begins, which in terms of atmospheric thermodynamics is the equilibrium level. The stratosphere is situated between about 10 km (6 mi) and 50 km (30 mi) altitude above the surface at moderate latitudes, while at the poles it starts at about 8 km (5 mi) altitude.

1.1.3 Mesosphere

The mesosphere extends from the stratopause to 80–85 km (50–53 mi; 260,000–280,000 ft). It is the layer where most meteors burn up upon entering the atmosphere. Temperature decreases with height in the mesosphere. The mesopause, the temperature minimum that marks the top of the mesosphere, is the coldest place on Earth and has an average temperature around −85 °C (−120 °F; 190 K)(States et al. 2000)

Joe Buchdahl, (2012) observed that at the mesopause, temperatures may drop to −100 °C (−150 °F; 170 K). Due to the cold temperature of the mesosphere, water vapor is frozen, forming ice clouds (or Noctilucent clouds). A type of lightning referred to as either sprites or ELVES, form many miles above thunderclouds in the troposphere.

1.1.4 Ionosphere

The Ionosphere is a part of the upper atmosphere, from about 85 km to 600 km altitude, comprising portions of the mesosphere, thermosphere and exosphere, distinguished because it is ionized by solar radiation. It plays an important part in atmospheric electricity and forms the inner edge of the magnetosphere. It has practical importance because, among other functions, it influences radio propagation to distant places on the Earth. (Rawer, 1993)

At heights of above 80 km (50 mi), in the thermosphere, the atmosphere is so thin that free electrons can exist for short periods of time before they are captured by a nearby positive ion. The number of these free electrons is sufficient to affect radio propagation. This portion of the atmosphere is *ionized* and contains plasma which is referred to as the ionosphere. In plasma, the negative free electrons and the positive ions are attracted to each other by the electromagnetic force, but they are too energetic to stay fixed together in an electrically neutral molecule.

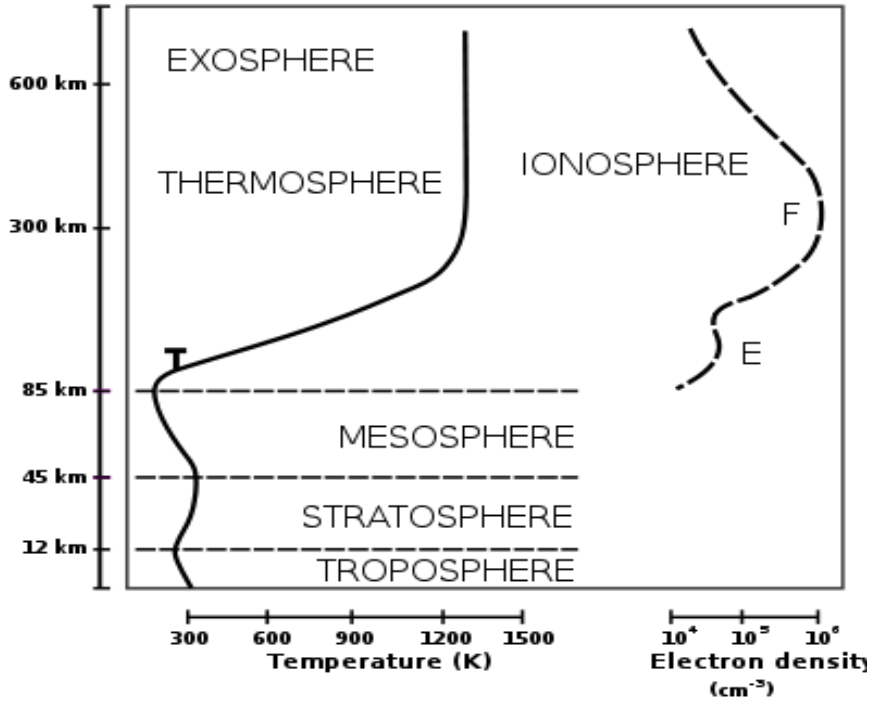

Figure 1.1 Relationship of the atmosphere and ionosphere (Wikipedia)

The ionosphere is a shell of electrons and electrically charged atoms and molecules that surrounds the Earth, stretching from a height of about 50 km to more than 1000 km. It owes its existence primarily to ultraviolet radiation from the Sun.

Ultraviolet (UV), X-Ray and shorter wavelengths of solar radiation are *ionizing*, since photons at these frequencies contain sufficient energy to dislodge an electron from a neutral gas atom or molecule upon absorption. In this process the light electron obtains a high velocity so that the temperature of the created electronic gas is much higher (of the order of thousand K) than the one of ions and neutrals. The reverse process to Ionization is recombination, in which a free

electron is "captured" by a positive ion, occurs spontaneously. This causes the emission of a photon carrying away the energy produced upon recombination. As gas density increases at lower altitudes, the recombination process prevails, since the gas molecules and ions are closer together. The balance between these two processes determines the quantity of ionization present.

Ionization depends primarily on the Sun and its activity. The amount of ionization in the ionosphere varies greatly with the amount of radiation received from the Sun. Thus there is a diurnal (time of day) effect and a seasonal effect. The local winter hemisphere is tipped away from the Sun, thus there is less received solar radiation. The activity of the Sun is associated with the sunspot cycle, with more radiation occurring with more sunspots. Radiation received also varies with geographical location (polar, aurora zones, mid-latitudes, and equatorial regions). There are also mechanisms that disturb the ionosphere and decrease the ionization. There are disturbances such as solar flares and the associated release of charged particles into the solar wind which reaches the Earth and interacts with its geomagnetic field.

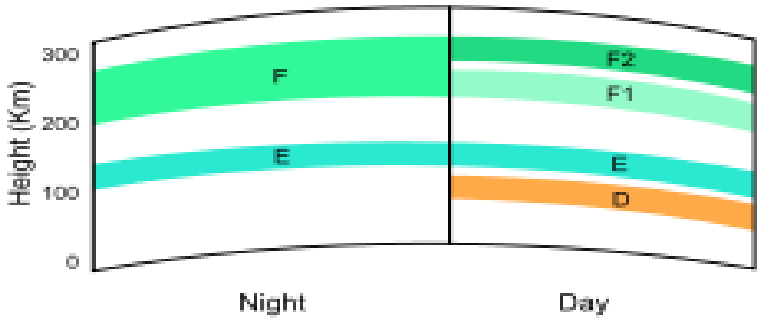

Figure 1.2 the Ionospheric Layers (Wikipedia)

At night the F layer is the only layer of significant ionization present, while the ionization in the E and D layers is extremely low. During the day, the D and E layers become much more heavily ionized, as does the F layer, which develops an additional, weaker region of ionization known as the F_1 layer. The F_2 layer persists by day and night and is the region mainly responsible for the refraction of radio waves.

1.2 Source of geomagnetic field

The Earth has a substantial magnetic field that is composed of contributions from many sources of which the most dominant is of core origin. The Earth's field consists of two main components; (i) The main field sometimes referred to as geomagnetic main field and (ii) the variation field.

The main field has its origin deep inside the Earth. Prior to this discovery, scientists attributed the main field of the Earth to the magnetization of rocks and the rotation of the Earth. From the recent research work, it has been discovered that the outer core of the Earth is made up of fluid while the inner core is solid composed principally of iron. Above the core are the mantles and the crust. It is also found that the major part of the magnetic field observed at the Earth's surface is created by the electric currents flowing in the core, which because of its metallic composition has electrical conductivity.

The electric current flowing in the Earth's interior, sets up magnetic field by induction. The process is maintained by some magneto-hydrodynamic phenomenon (this implies that the motion of electrons or the fluid core generates flow of current and in turn magnetic field are set up which again as the flow continues induced magnetism along the neighboring rocks). This mechanism is sometimes termed the dynamo effect. At the Earth's surface the form of the geomagnetic field is similar to the field around a bar magnet (dipolar).

Variation field is related to source in the upper atmosphere that is associated with induced current in the Earth. Contribution to the Earth's field could be explained by atmospheric dynamo actions sometimes refer to as Ionospheric dynamo action. The Earth's magnetosphere protects from most harmful radiations from the sun.

1.3 Geomagnetic Components

The direction and strength of the magnetic field can be measured at the surface of the Earth and plotted. Since geomagnetic field is a vector field, at least three elements (components) are necessary to represent the field. The elements describing the direction of the field are declination (**D**) and inclination (**I**). **D** and **I** are measured in units of degrees. **D** is the angle between

magnetic north and true north and positive when the angle measured is east of true north and negative when west. **I** is the angle between the horizontal plane and the total field vector.

Elements describing the field intensity are the total intensity (**F**), horizontal component (**H**), vertical component (**Z**), and the north (**X**) and east (**Y**) components of the horizontal intensity. These elements are generally expressed in units of NanoTesla (10^{-9} Tesla / 10^{-5} Gauss or 1 Gamma in CGS). Combinations of the three elements frequently used in geomagnetism are HDZ, XYZ and FDI. Principal equations relating the values of the elements are as follows:

(a) Declination (D) = Tan^{-1} (Y/X)
(b) Inclination (I) = Tan^{-1} (Z/H)
(c) Horizontal (H) = $\sqrt{(X^2 + Y^2)}$
(d) North (X) = H*Cos (D)
(e) East (Y) = H*Sin (D)
(f) Intensity (F) = $\sqrt{(X^2 + Y^2 + Z^2)}$ **(1.1)**

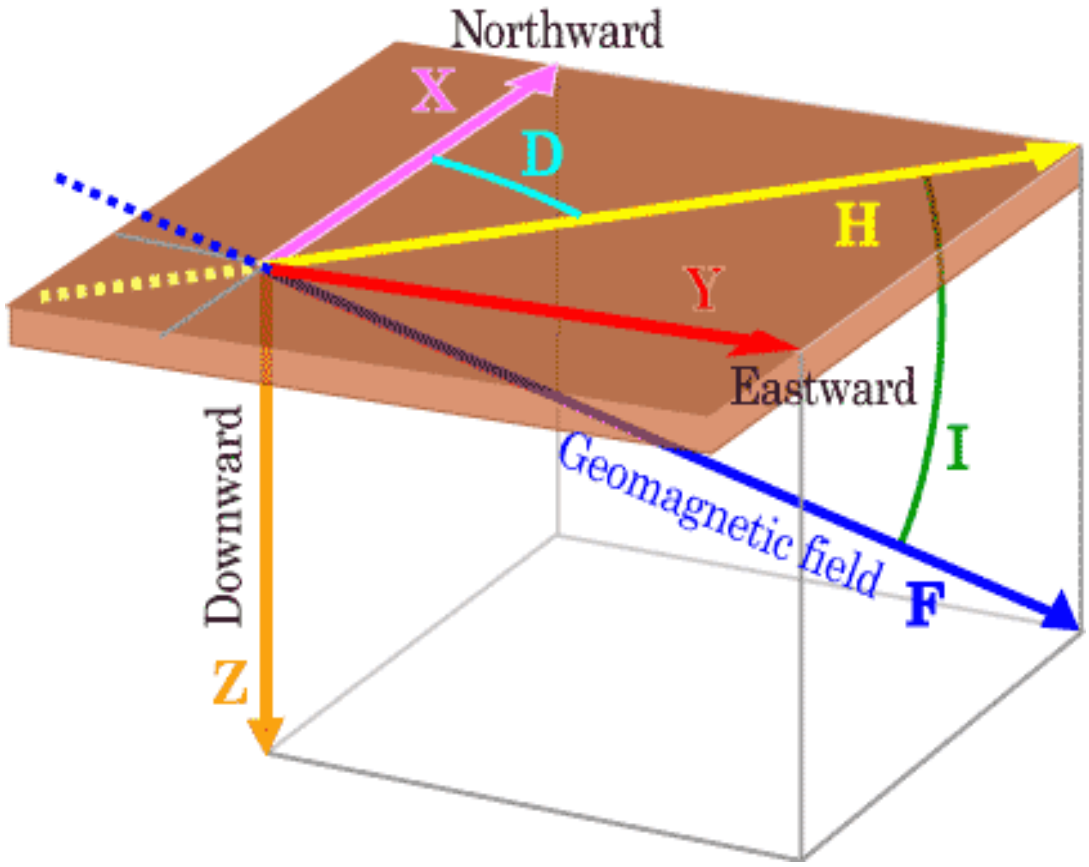

Figure 1.3 Geomagnetic field components (Curled from WDC for Geomagnetism Kyoto)

1.4 Geomagnetic field variations

The geomagnetic field changes on time scales from milliseconds to millions of years. Shorter time scales mostly arise from currents in the ionosphere and magnetosphere, and some changes can be traced to geomagnetic storms or daily variations in currents. Changes over time scales of a year or more mostly reflect changes in the Earth's interior, particularly the iron-rich core.

Frequently, the Earth's magnetosphere is hit by solar flares causing geomagnetic storms, provoking displays of auroras. The short-term instability of the magnetic field is measured with the K-index.

The intensity and structure of the Earth's magnetic field are always changing, slowly but erratically, reflecting the influence of the flow of thermal currents within the iron core. This variation is reflected in part by the wandering of the North and South Geomagnetic Poles. Because a wide range of commercial and military navigation and attitude/heading systems are dependent on models of the magnetic field, these models need to be updated periodically.

1.5 Annual and Semi-annual variations in geomagnetic activity

The Earth’s magnetic field exhibits short and long term variations, ranging from seconds to many millions of years. Observations of the geomagnetic field allow separation of these temporal variations into two main categories, depending on their origin: external and internal, with respect to the terrestrial surface.

Variations on short time scales are usually attributed to the external sources, because the conductive mantle screens out high frequency variations arising in the core. The variability of the external field variation, in fact the geomagnetic activity, is due to the response of the Earth’s ionosphere and magnetosphere to the solar activity, variation of the solar wind speed and fluctuation of the Interplanetary Magnetic Field.

The magnetosphere of Earth is a region in space whose shape is determined by the Earth's internal magnetic field, the solar wind plasma, and the interplanetary magnetic field (IMF). In the magnetosphere, a mix of free ions and electrons from both the solar wind and the Earth's

ionosphere is confined by electromagnetic forces that are much stronger than gravity and collisions.

Despite its name, the magnetosphere is distinctly non-spherical. All known planetary magnetospheres in the solar system possess more of an oval tear-drop shape because of the solar wind.

The upward extension of the ionosphere, known as the plasmasphere, also extends beyond 4-5 R_E with diminishing density, beyond which it becomes a flow of light ions called the polar wind that escapes out of the magnetosphere into the solar wind. Energy deposited in the ionosphere by auroras strongly heats the heavier atmospheric components such as oxygen and molecules of oxygen and nitrogen, which would not otherwise escape from Earth's gravity. Owing to this highly variable heating, however, a heavy atmospheric or ionospheric outflow of plasma flows during disturbed periods from the auroral zones into the magnetosphere, extending the region dominated by terrestrial material, known as the fourth or plasma geosphere, at times out to the magnetopause.

Earth’s magnetosphere provides protection, without which life as we know it could not survive. Mars, with little or no magnetic field is thought to have lost much of its former oceans and atmosphere to space in part due to the direct impact of the solar wind. Venus with its thick atmosphere is thought to have lost most of its water to space in large part owing to solar wind ablation. (NASA, 2009)

Due to the size of Jupiter's magnetosphere there is a possibility of very weak and very brief seasonal head-tail interaction between Earth's and Jupiter's magnetospheres. The magnetospheres of the outer gas planets may weakly interact, although their magnetospheres are much smaller than Jupiter's.

1.6 Geomagnetism and related phenomenon

1.6.1 Geomagnetic storms

A geomagnetic storm is a temporary disturbance of the Earth's magnetosphere caused by a disturbance in the interplanetary medium. A geomagnetic Storm is a major component of space weather and provides the input for many other components of space weather.

Geomagnetic storms are caused by solar wind shock wave and/or cloud of magnetic field which interact with the Earth's magnetic field. The increase in the solar wind pressure initially compresses the magnetosphere and the solar wind magnetic field will interact with the Earth's magnetic field and transfer an increased amount of energy into the magnetosphere. Both interactions cause an increase in movement of plasma through the magnetosphere (driven by increased electric fields inside the magnetosphere) and an increase in electric current in the magnetosphere and ionosphere.

During the main phase of a geomagnetic storm, electric current in the magnetosphere create magnetic force which pushes out the boundary between the magnetosphere and the solar wind. The disturbance in the interplanetary medium which drives the geomagnetic storm may be due to a solar coronal mass ejection (CME) or a high speed stream (co-rotating interaction region or CIR) of the solar wind originating from a region of weak magnetic field on the Sun's surface. The frequency of geomagnetic storms increases and decreases with the Sunspot cycle, CME driven storms are more common during the maximum of the solar cycle and CIR driven storms are more common during the minimum of the solar cycle.

A geomagnetic storm can also be defined by changes in the DST (disturbance – storm time) index (Gonzalez et al. 1994). The DST index estimates the globally averaged change of the horizontal component of the Earth's magnetic field at the magnetic equator based on measurements from a few magnetometer stations. DST is computed once per hour and reported in near-real-time (Siguira et al. 1991). During quiet times, DST is between +20 and -20 nano-Tesla (nT).

The size of a geomagnetic storm is classified as moderate (-50 nT >minimum of Dst > -100 nT), intense (-100 nT > minimum Dst > -250 nT) or super-storm (minimum of Dst < -250 nT).

1.6.2 Sunspots

Sunspots are temporary phenomena on the photosphere of the Sun that appear visibly as dark spots compared to surrounding regions. They are caused by intense magnetic activity, which inhibits convection by an effect comparable to the eddy current brake, forming areas of reduced surface temperature. Like magnets, they also have two poles. Although they are at temperatures

of roughly 3000 – 4500 K (2727 – 4227 °C), the contrast with the surrounding material at about 5,780 K leaves them clearly visible as dark spots, as the luminous intensity of a heated black body (closely approximated by the photosphere) is a function of temperature to the fourth power. If the sunspot were isolated from the surrounding photosphere it would be brighter than an electric arc. Sunspots expand and contract as they move across the surface of the Sun and can be as large as 80,000 kilometers (50,000 mi) in diameter, making the larger ones visible from Earth without the aid of a telescope. They may also travel at relative speeds ("proper motions") of a few hundred m/s when they first emerge onto the solar photosphere.

1.6.3 Solar Flare

A solar flare is a sudden brightening observed over the Sun surface or the solar limb, which is interpreted as a large energy release of up to 6×10^{25} joules of energy (about a sixth of the total energy output of the Sun each second) (kopp et al. 2005). The flare ejects clouds of electrons, ions, and atoms through the corona into space. These clouds typically reach the earth a day or two after the event. The term is also used to refer to similar phenomena in other stars, where the term stellar flare applies (Menzel et al. 1970).

Solar flares affect all layers of the solar atmosphere (photosphere, chromosphere, and corona), when the medium plasma is heated to tens of millions of Kelvin’s and electrons, protons, and heavier ions are accelerated to near the speed of light. They produce radiation across the electromagnetic spectrum at all wavelengths, from radio waves to gamma rays, although most of the energy goes to frequencies outside the visual range and for this reason the majority of the flares are not visible to the naked eye and must be observed with special instruments. Flares occur in active regions around sunspots, where intense magnetic fields penetrate the photosphere to link the corona to the solar interior. Flares are powered by the sudden (timescales of minutes to tens of minutes) release of magnetic energy stored in the corona. The same energy releases may produce coronal mass ejections (CME), although the relation between CMEs and flares is still not well established.

X-rays and UV radiation emitted by solar flares can affect Earth's ionosphere and disrupt long-range radio communications. Direct radio emission at decimetric wavelengths may disturb operation of radars and other devices operating at these frequencies.

The frequency of occurrence of solar flares varies, from several per day when the Sun is particularly "active" to less than one every week when the Sun is "quiet", following the 11-year cycle (the solar cycle). Large flares are less frequent than smaller ones.

1.6.4 CME's

A coronal mass ejection (CME) is a massive burst of solar wind and magnetic fields rising above the solar corona or being released into space.

Coronal mass ejections are often associated with other forms of solar activity, most notably solar flares, but a causal relationship has not been established. Most ejections originate from active regions on Sun's surface, such as groupings of sunspots associated with frequent flares. Near solar maxima the Sun produces about three CMEs every day, whereas near solar minima there is about one CME every five days (Nicky Fox, 2011).

Coronal mass ejections release huge quantities of matter and electromagnetic radiation into space above the sun's surface, either near the corona (sometimes called a solar prominence) or farther into the planet system or beyond (interplanetary CME). The ejected material is a plasma consisting primarily of electrons and protons, but may contain small quantities of heavier elements such as helium, oxygen, and even iron. It is associated with enormous changes and disturbances in the coronal magnetic field. Coronal mass ejections are usually observed with a white-light coronagraph.

1.6.5 IMF

The interplanetary magnetic field (IMF) is the term for the solar magnetic field carried by the solar wind between the planets of the Solar System. The solar wind is a plasma, thus it has the characteristics of a plasma, for example, it is highly electrically conductive so that magnetic field lines from the Sun are carried along with the wind. The dynamic pressure of the wind dominates over the magnetic pressure through most of the solar system (or heliosphere), so that the magnetic field is pulled into an Archimedean spiral pattern (the Parker spiral) by the combination of the outward motion and the Sun's rotation. Depending on the hemisphere and phase of the solar cycle, the magnetic field spirals inward or outward; the magnetic field follows the same

shape of spiral in the northern and southern parts of the heliosphere, but with opposite field direction. These two magnetic domains are separated by a two current sheet (an electric current that is confined to a curved plane). This heliospheric current sheet has a shape similar to a twirled ballerina skirt, and changes in shape through the solar cycle as the Sun's magnetic field reverses about every 11 years.

The plasma in the interplanetary medium is also responsible for the strength of the Sun's magnetic field at the orbit of the Earth being over 100 times greater than originally anticipated. If space were a vacuum, then the Sun's 10^{-4} tesla magnetic dipole field would reduce with the cube of the distance to about 10^{-11} tesla. But satellite observations show that it is about 100 times greater at around 10^{-9} tesla. Magneto-hydrodynamic (MHD) theory predicts that the motion of a conducting fluid (e.g. the interplanetary medium) in a magnetic field induces electric currents, which in turn generates magnetic fields, and in this respect it behaves like a MHD dynamo.

1.7 Purpose of Study

The purpose of this study is as follows:

1. To present for the first time (from available literature) the use of the difference in the field strength for all days of the year and Sq days in identifying annual and semiannual variation in the geomagnetic activity. Previous analysis have either used geomagnetic activity indices [such as aa and ap (e.g Bartels 1932, Cliver et al. 2002, Le Mouel et al., 2004), kp data (Chulliat et al. 2005) and inter hourly variation (Svalgaard and Cliver, 2007)]; and amplitude of the diurnal geomagnetic variation, and consequently inferring the mechanism of the solar heliospheric modulation of the geomagnetic activity.
2. To present a brief result of the latitudinal profile of the association between solar activity and the geomagnetic field strength.

CHAPTER TWO

LITERATURE REVIEW

2.1 Annual variation of geomagnetic field components

The influence of the heliosphere on the variation of the geomagnetic field on annual and semiannual scales have been studied by many authors using geomagnetic activity indices (e.g. McIntosh 1959, Russell and McPherron 1973, Svalgaard, 1977, Cliver et al. 2002, Mursula et al. 2011), amplitudes of solar quiet day (Sq) variation (e.g. Rastogi et al 1994 ,Wardinski and Mandea 2006, Yamazaki and Yumoto 2012) mean monthly/yearly values of geomagnetic components (Rao and Bansal (1969), Wardinski and Mandea 2006, Bhardwaj and Rao, 2013). The semiannual variation of mid latitude geomagnetic activity is generally attributed to the Russell-McPherron (RM) effect (Russell and McPherron 1973) which predicts a six-month cycle in the Bz component of the solar wind magnetic field in geocentric solar magnetospheric secondary cause such that when the earth is North(or South) of the solar equator, a more active northern (or southern) hemisphere would result in a stronger and faster solar wind causing enhanced geomagnetic activity (Mursala et al., 2011). Svalgaad (2011) however observed no oppositely organized annual variations in the solar driver of geomagnetic activity nor in the observed activity in step with the alternating cycle polarities.

Local magnetic observations show an annual variation of the geomagnetic activity, such as storms, sub-storms and auroras, which have been related to the annual change in solar illumination (Courtillot and LeMou¨el, 1988) and a variation of solar wind speed due to the change of the heliographic latitude of the Earth (Bolton, 1990; Zieger and Mursula, 1998). The annual variation was also found in the long-term occurrence of auroras (Silverman and Shapiro, 1983).

In a series of papers (Malin and Isikara, 1976; Malin and Winch, 1996; Malin *et al.*, 1999) the mechanism for the annual variation of the geomagnetic field was outlined. This variation divides into two parts: an annual non-ionospheric and an independent part resulting from the seasonal modulation of Sq. The non-ionospheric term is related to the movement of the ring current towards the winter hemisphere due to the presence of the solar wind.

2.2 Semiannual variation of geomagnetic field components

A significant influence of solar activity on the semiannual Sq variation was suggested by Rastogi et al. (1994) to explain the linear relationship between the yearly averaged Sq range and the amplitude of the semiannual Sq variations at the dip-equatorial latitudes. The annual north and south migration of the ring current would cause the current to pass directly over a low latitude observatory twice a year resulting in a semiannual variation of geomagnetic field components (Malin et al., 1999). Yamazaki and Yumoto (2012) equally observed positive correlation between annual and semiannual Sq variations and sunspot number. Bhardwaj and Subba Rao (2013) observed that the residuals of geomagnetic elements D, H and Z at six indian geomagnetic observatories using annual and monthly mean values do not show any parallelism with the 11 year sunspot cycle, but showed periodicities of 2-3 solar cycles.

(Malin *et al.*, 1999; Balan *et al.*, 2000) observed that the semi-annual variation of the geomagnetic field, and that of the geomagnetic activity have extrema near the equinoxes suggesting a common origin. It was also observed that the semi-annual variation is due to changes in the intensity of the ring current, as a consequence of the so-called Russell-McPherron effect (Russell and McPherron, 1973), where the magnetosphere is more efficient at trapping particles at certain times (twice in the year), because of the favorable geometry of the solar wind and magnetosphere.

Okeke and Hamano (2000) analyzed hourly mean values which were used to study the variations in D, H & Z components at new equatorial electrojet regions. The analysis revealed the following;

(i) That the amplitude of *dH* has diurnal variation which peaks during the day at about local noon in all the three equatorial electrojet regions.
(ii) Diurnal variation was observed in *D* which indicates that the equatorial electrojet current system has both east-west and north-south components.
(iii) The pronounced magnitude of *Z* variation was observed in Kiritimati which was attributed mainly to sea induction.
(iv) Seasonal variations with more pronounced equinoctial maximum were observed in *H* than in *Z*.
(v) *D* component showed no consistent seasonal variation in all the regions.
(vi) The equinoctial maximum is due to enhanced equatorial electron density at equinox.

Wardinski and Mandea, (2006) observed that the semi-annual peak was clearly better detected in the horizontal components for the observatories situated in the equatorial region, which is related to Russell-McPherron effect (Russell and McPherron, 1973) due to the favorable geometry between solar wind and magnetosphere. While the effect mainly explains periodicity in geomagnetic activity, it also affects the intensity of the ever-present ring current. For observatories in mid and high-latitudes both peaks were well detected in horizontal components. There study also showed the existence of a possible correlation of the annual variation in Europe and the semiannual variation in North America with the mantle conductivity of the two regions.

Yamazaki *et al*., (2011) constructed an empirical model of the quiet daily geomagnetic field variation based on geomagnetic data obtained from 21 stations along the 210 Magnetic Meridian of the Circum-pan Pacific Magnetometer Network (CPMN) from 1996 to 2007. They found out three particularly noteworthy results. First, the total current intensity of the Solar quiet daily variation (S) current system is largely controlled by solar activity while its focus position is not significantly affected by solar activity. Second, they found that seasonal variations of the S current intensity exhibit north-south asymmetry; the current intensity of the northern vortex shows a prominent annual variation while the southern vortex shows a clear semi‑annual variation as well as annual variation. Thirdly, they found that the total intensity of the Lunar quiet daily variations (L) current system changes depending on solar activity and season; seasonal variations of the L current intensity show an enhancement during the December solstice, independent of the level of solar activity.

De Michelis *et al*., (2010) analyzed the hourly means of the magnetic elements H, D and Z recorded at L'Aquila observatory in Italy from 1993 to 2004. They applied to the dataset, the NOC technique to reconstruct the 3- dimensional structures of the different ionospheric and magnetospheric current systems which contribute to the geomagnetic daily variations.
They observed that the principal contributions to the geomagnetic daily variations are related to: (a) the ionospheric currents, (b) the current system in the ionosphere and magnetosphere corresponding to the partial wind current and the related field-alligned currents and (c) the magnetopause current

CHAPTER THREE

METHOD OF ANALYSIS AND RESULTS

3.1 Source of Data on Geomagnetic Field Components

Ten stations were employed in carrying out the study of annual and semiannual variation of geomagnetic field components. The Hourly Data for the geomagnetic field of the DHZ or XYZ components were obtained from World datacenter for Geomagnetism, Kyoto Japan, where geomagnetic data from around the earth were recorded.

Computations were made to obtain the H, D and Z values from the equation introduced in section 1.3.

All the observatories lie in the Northern Hemisphere cutting across many latitudes. Table 3.1 shows the observatories with their geographic and geomagnetic coordinates.

3.2 Sources of Dst. data, sunspot, aa-index and F10.7 data

Dst Index values were gotten from World Data Center for Geomagnetism, Kyoto Japan (http://wdc.kugi.kyoto-u.ac.jp/index.html) while Sunspot number data were gotten from National aeronautics and space administration (http://solarscience.msfc.nasa.gov/SunspotCycle.shtml). Aa-index Data were gotten from Space Physics Interactive Data Resource, SPIDR(http://spidr.ngdc.noaa.gov/spidr), while Solar Flux Data were gotten from National Geographical Data Center, NGDC (http://www.ngdc.noaa.gov).

Table 3.1 Geographic and Geomagnetic location of stations

Stations	IAGA Code	Geographic latitude (^{O}N)	Geographic longitude (^{O}E)	Geomagnetic latitude (^{O}N)
Guam	GUA	13.59	144.87	5.48
Alibag	ABG	18.64	72.87	10.26
San Juan	SJG	18.11	-66.15	27.92
Boulder	BOU	40.13	-105.24	48.05
Chambon-la-Foret	CLF	48.03	2.26	49.56
Belsk	BEL	51.84	20.79	50.06
Wingst	WNG	53.74	9.07	53.89
Sodankyla	SOD	67.37	26.63	63.87
Abisko	ABK	68.36	18.82	65.98
Barrow	BRW	71.32	-156.62	69.68

3.3 Data Analysis

The main criterion in data selection was the length and continuity of time series of the geomagnetic field components. We examined observatory data over a period of 24 years from 1985 to 2008 (cycles 22 and 23). Monthly means for each station were computed from hourly data acquired from these observatories, while the annual means were computed from the monthly means.

$$\text{(a) } D = \frac{\sum_{i=1}^{n} D_i}{n}, \qquad \text{(b) } H = \frac{\sum_{i=1}^{n} H_i}{n}, \qquad \text{(c) } Z = \frac{\sum_{i=1}^{n} Z_i}{n}$$

$$\text{(d) } D_q = \frac{\sum_{i=1,j=1}^{m,k} D_{ij}}{n} \qquad \text{(e) } H_q = \frac{\sum_{i=1,j=1}^{m,k} H_{ij}}{n}, \qquad \text{(f) } Z_q = \frac{\sum_{i=1,j=1}^{m,k} Z_{ij}}{n} \qquad \textbf{(3.1)}$$

n = 365/366days, m = 12months, k = 5days. D_i, H_i, Z_i is the $_i$th day of the D, H and Z component respectively while D_{ij}, H_{ij}, Z_{ij} represents the $_i$th day of a $_j$th month of the D_q, H_q and Z_q respectively.

$$\text{(a) } d = \frac{\sum_{i=1}^{n} d_i}{n} \qquad \text{(b) } h = \frac{\sum_{i=1}^{n} h_i}{n} \qquad \text{(c) } z = \frac{\sum_{i=1}^{n} z_i}{n}$$

$$\text{(d) } dq = \frac{\sum_{j=1}^{k} d_j}{5} \qquad \text{(e) } hq = \frac{\sum_{j=1}^{k} h_j}{5} \qquad \text{(f) } zq = \frac{\sum_{j=1}^{k} z_j}{5} \qquad \textbf{(3.2)}$$

n= 28/29/30/31days, k= 5days, d_i, h_i, z_i is the $_i$th day of the d, h and z component respectively while d_j, h_j, z_j are the $_j$th quietest day of the d_q, h_q and z_q respectively. The d, h, z, d_q, h_q, z_q are average over the period of 24 years.

(a) $D_{diff} = D - D_q$ (d) $d_{diff} = d - d_q$

(b) $H_{diff} = H - H_q$ (e) $h_{diff} = h - h_q$

(c) $Z_{diff} = Z - Z_q$ (f) $z_{diff} = z - z_q$ **(3.3)**

D, H and Z represent the annual mean for all the days, while D_q, H_q and Z_q represent the annual mean of the first 5quietest days for all the months in a given year. d, h, z represent the monthly

mean for all the days, while d_q, h_q, z_q represent the monthly mean of the first 5 quietest days for all the months in a given year.

From Equation (3.3) Six parameters representing annual (D_{diff}, H_{diff} and Z_{diff}) and monthly (d_{diff}, h_{diff} and z_{diff}) residuals of the geomagnetic field were defined, and presented as indicators of ring current monthly/yearly influence on the strength of the geomagnetic field components. The ring current on the geomagnetic field strength was used to determine the annual and semiannual geomagnetic activity variation and validate Russell-McPherron hypothesis. The plot of the annual variation (D_{diff}, H_{diff} and Z_{diff}) is shown in figure 3.1 to 3.9 for low, mid and high latitude stations. The semiannual (seasonal) variation of the derived quantities-d_{diff}, h_{diff} and z_{diff} is presented in figure 3.10 to 3.18 for low, mid and high latitude stations. Pearson correlation coefficients between sunspot number/Dst and D_{diff}, H_{diff}, Z_{diff} for each station were obtained; the latitudinal profile is shown in figure 3.22.

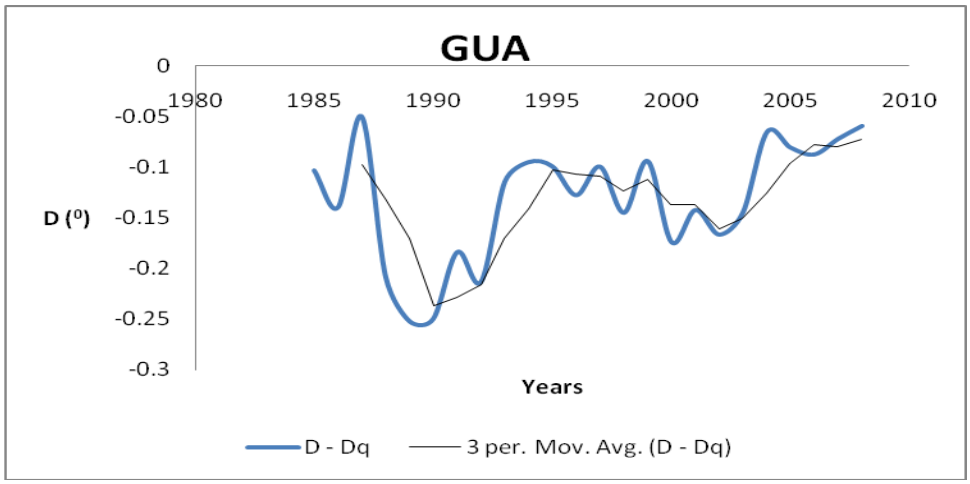

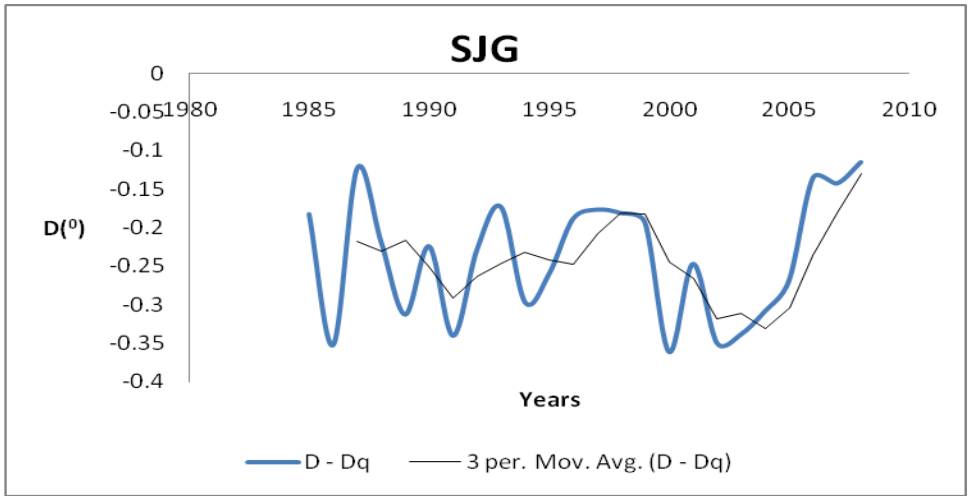

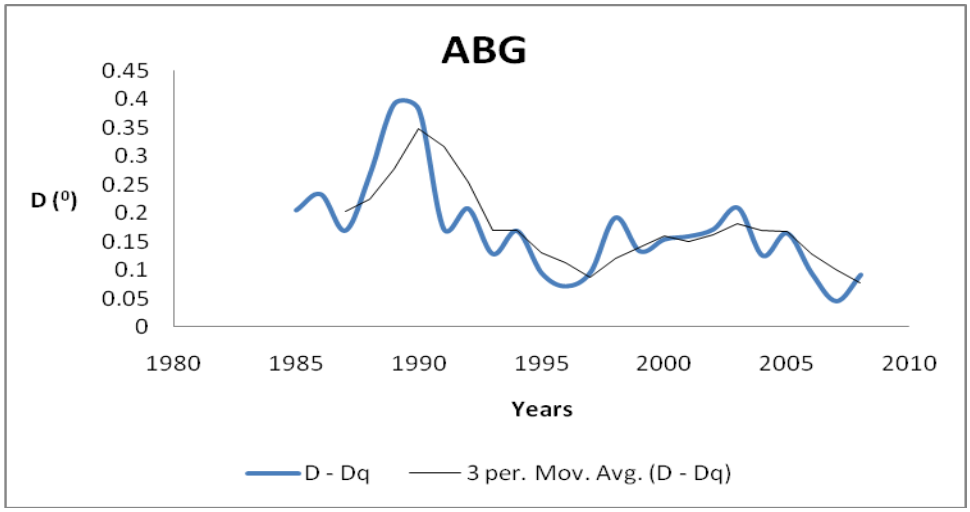

Figure 3.1 D_{diff} for geomagnetic low latitude stations

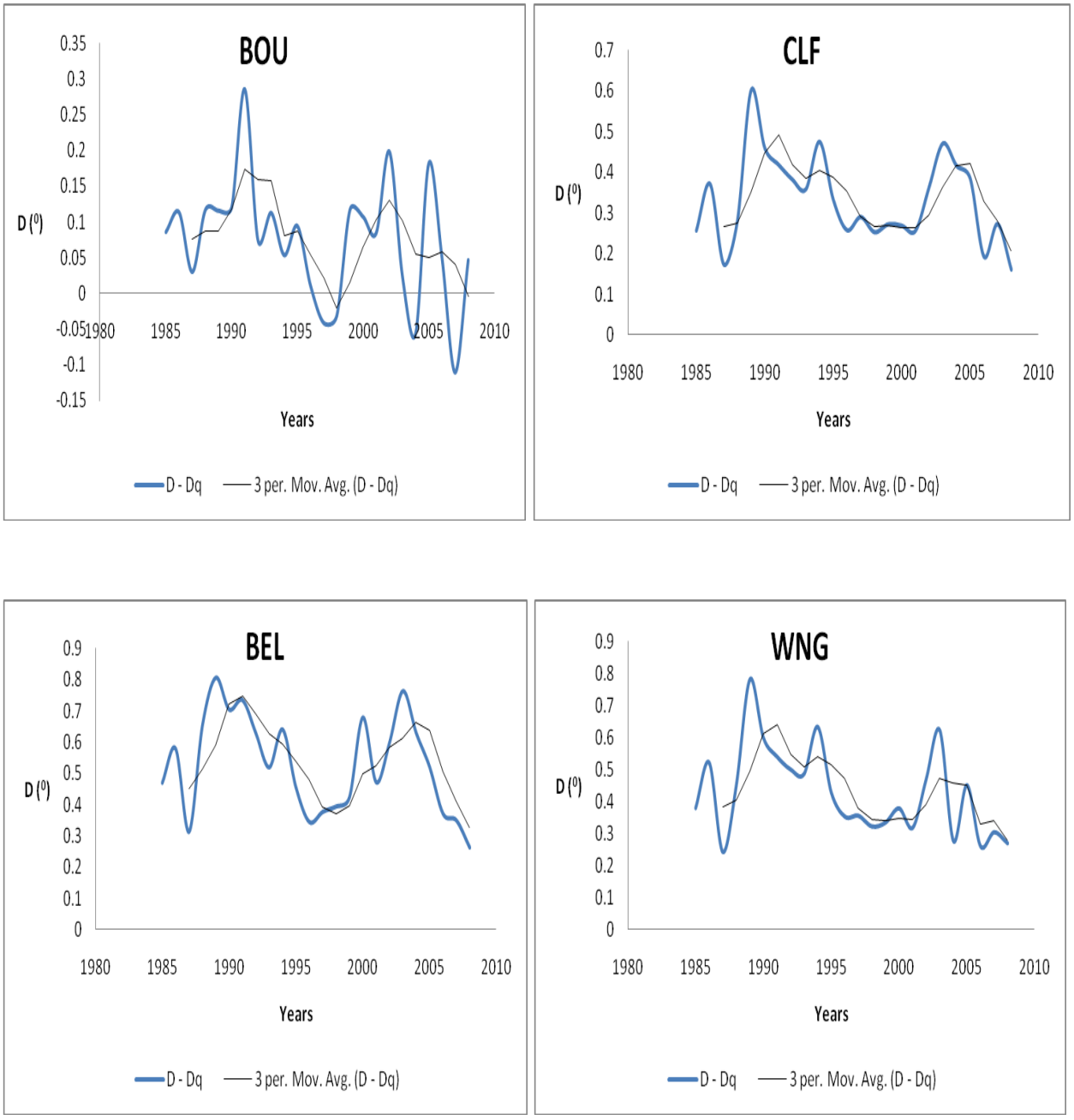

Figure 3.2 D_{diff} for geomagnetic mid latitude stations

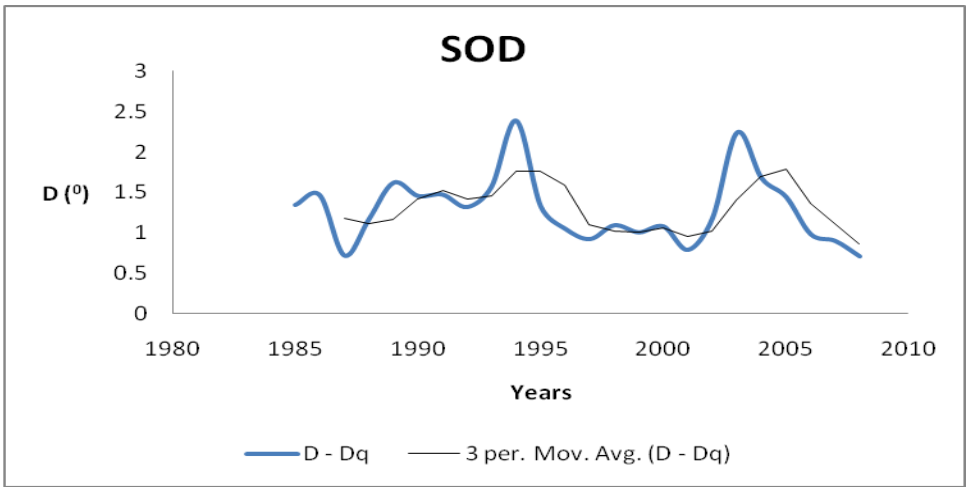

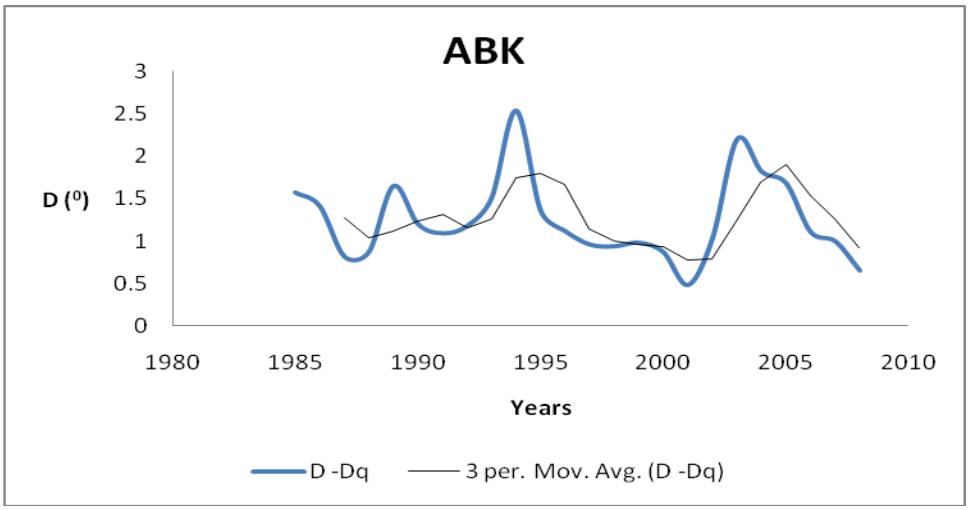

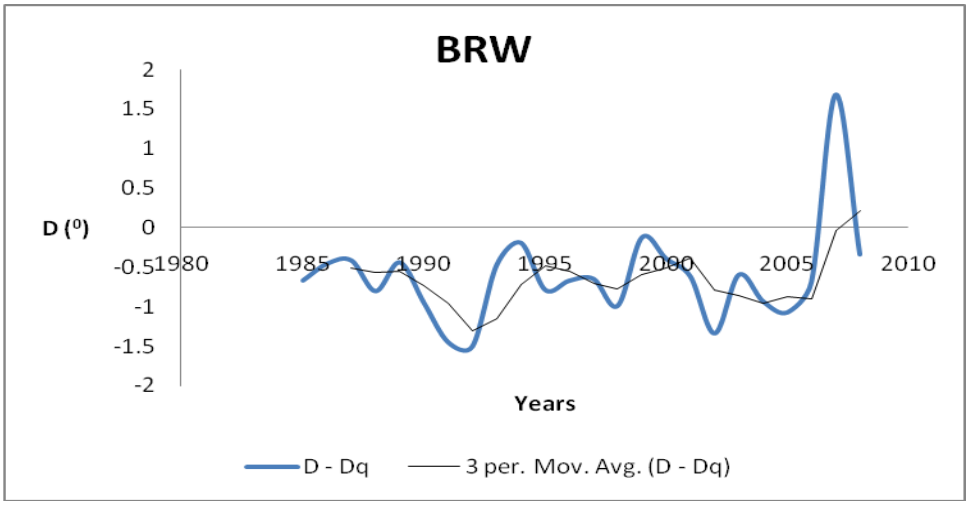

Figure 3.3 D_{diff} for geomagnetic high latitude stations

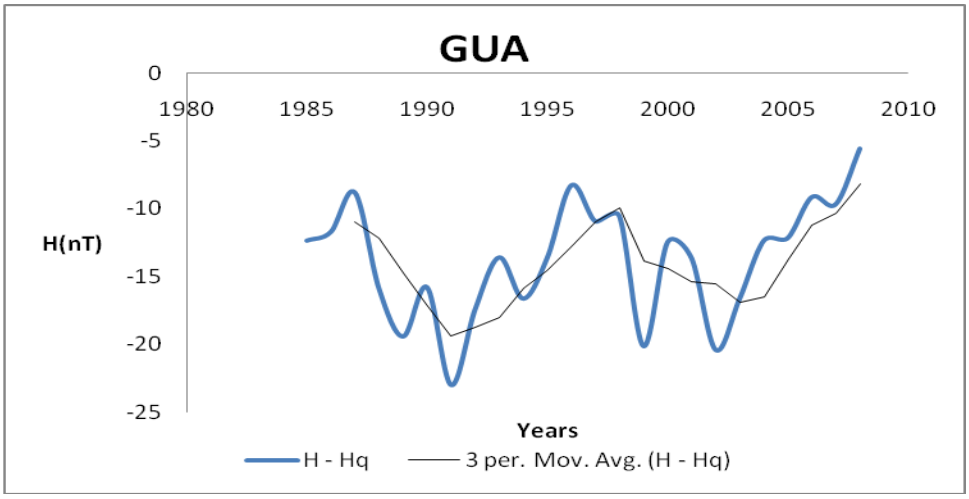

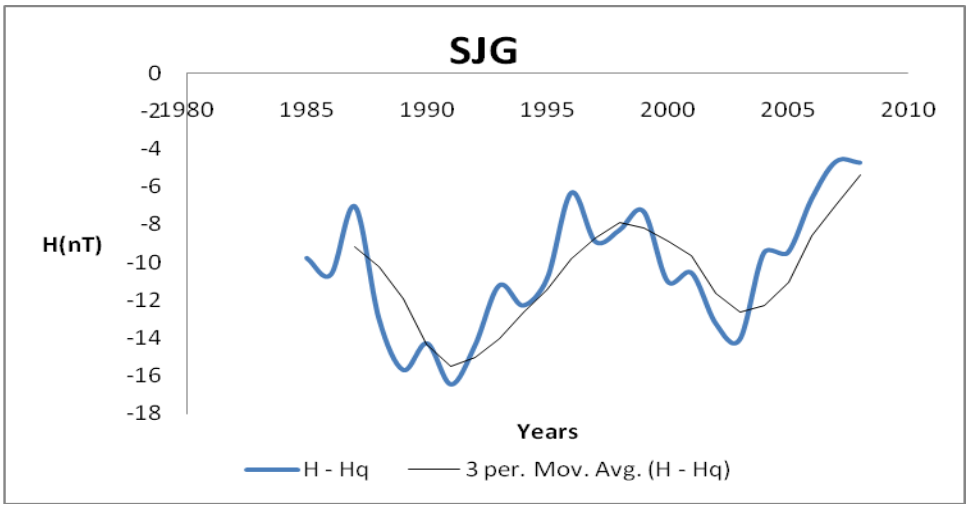

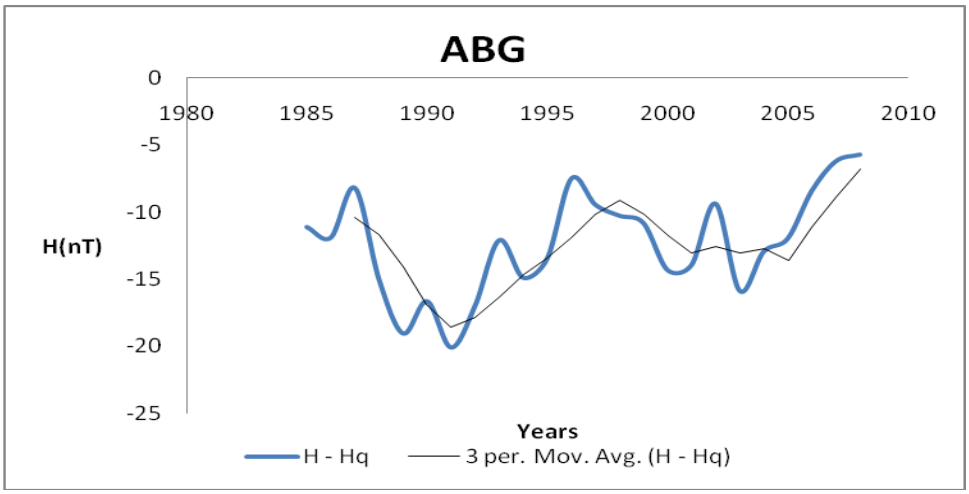

Figure 3.4 H_{diff} for geomagnetic low latitude stations

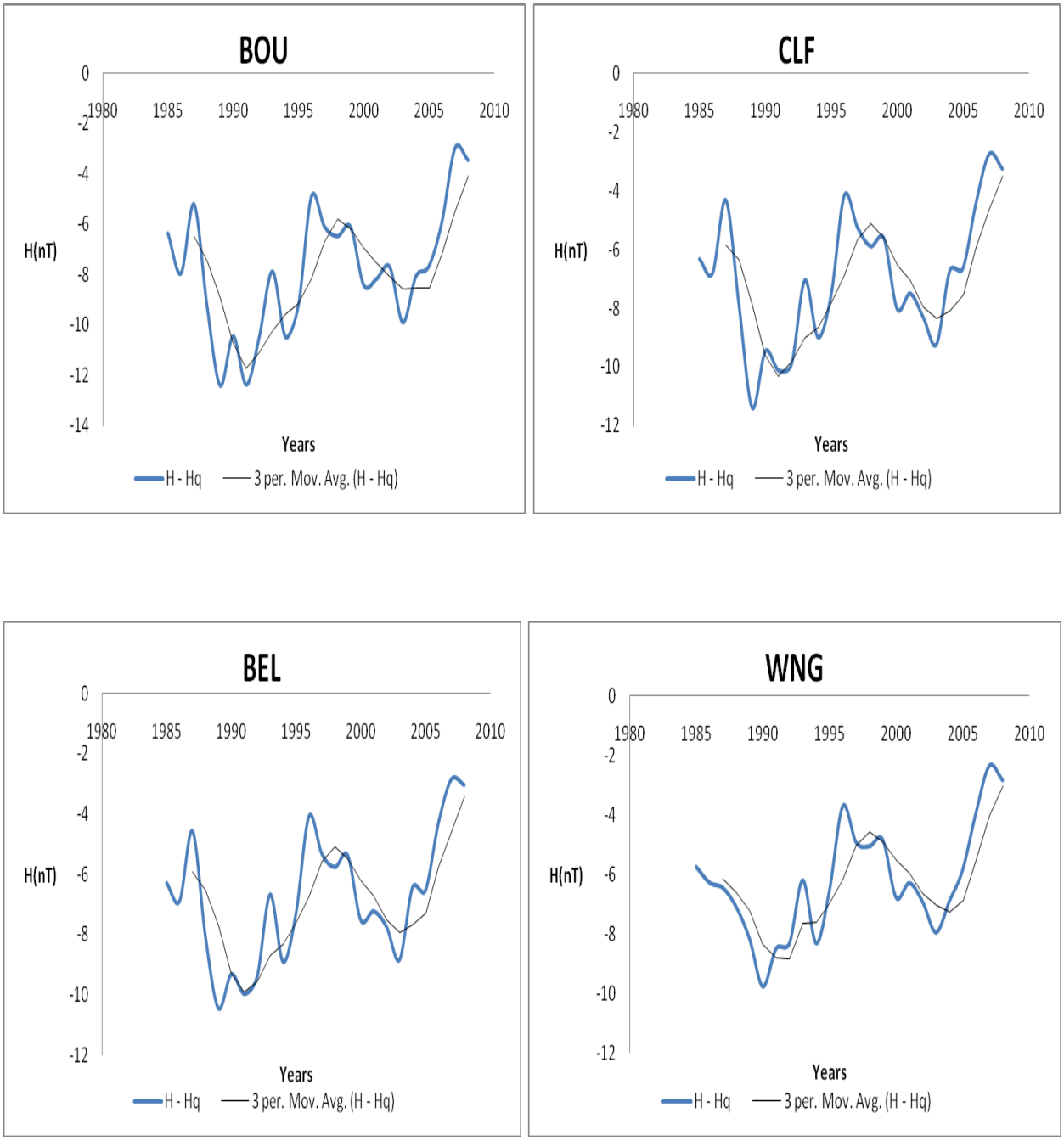

Figure 3.5 H_{diff} for geomagnetic mid latitude stations

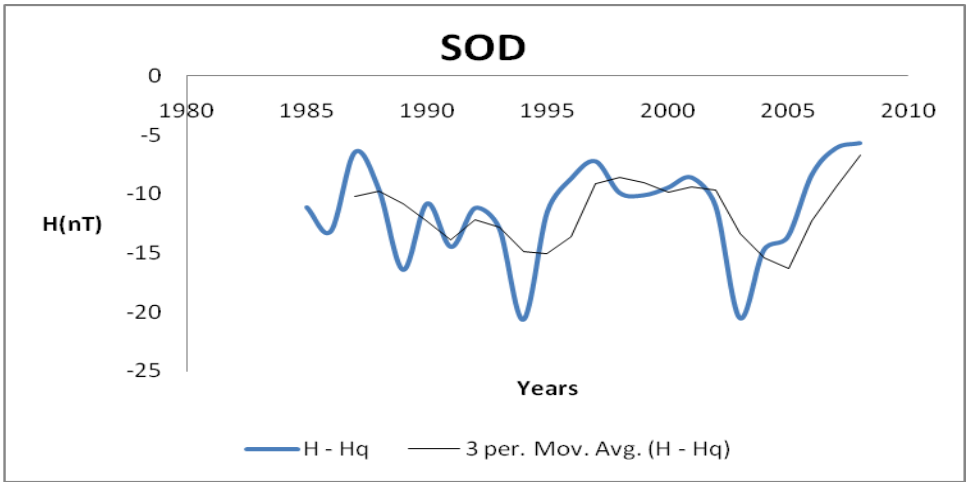

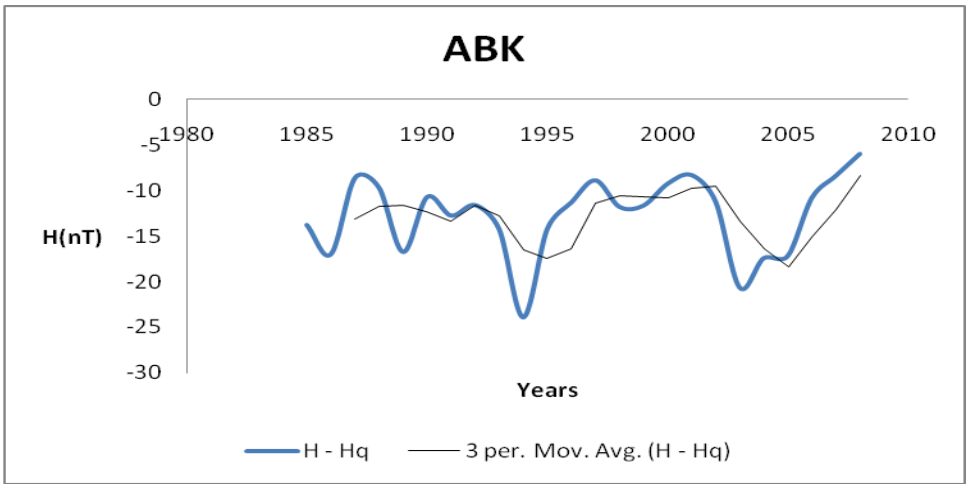

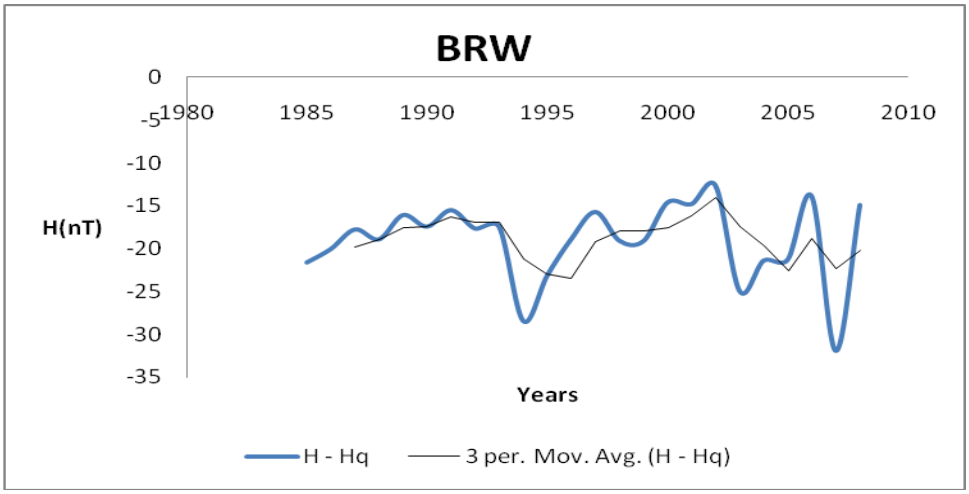

Figure 3.6 H_{diff} for geomagnetic high latitude stations

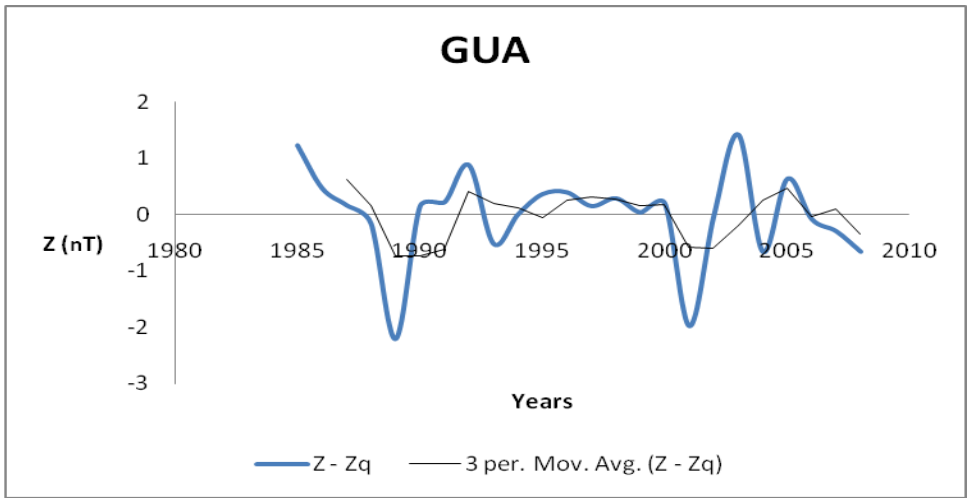

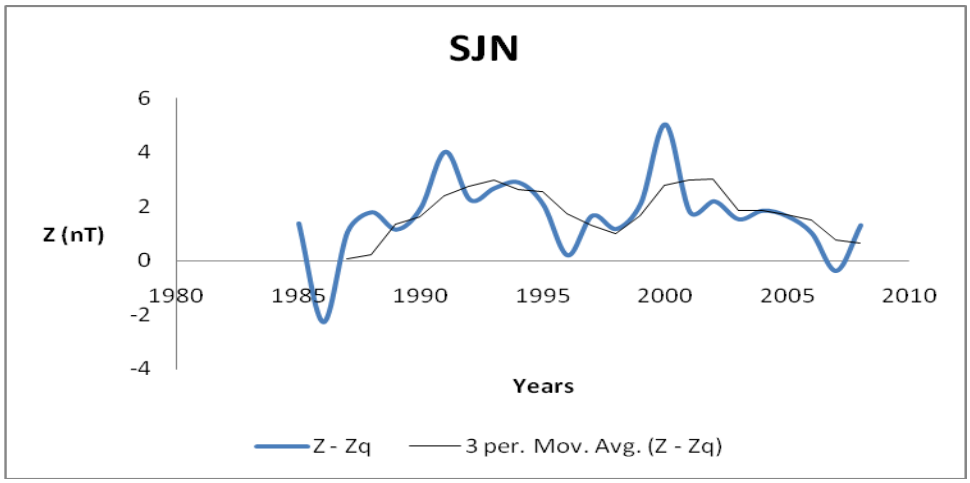

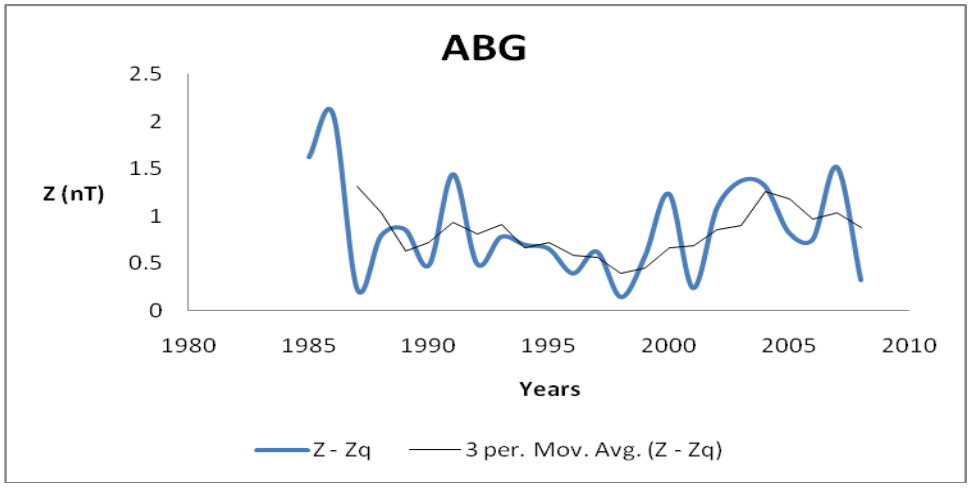

Figure 3.7 Z_{diff} for geomagnetic low latitude stations

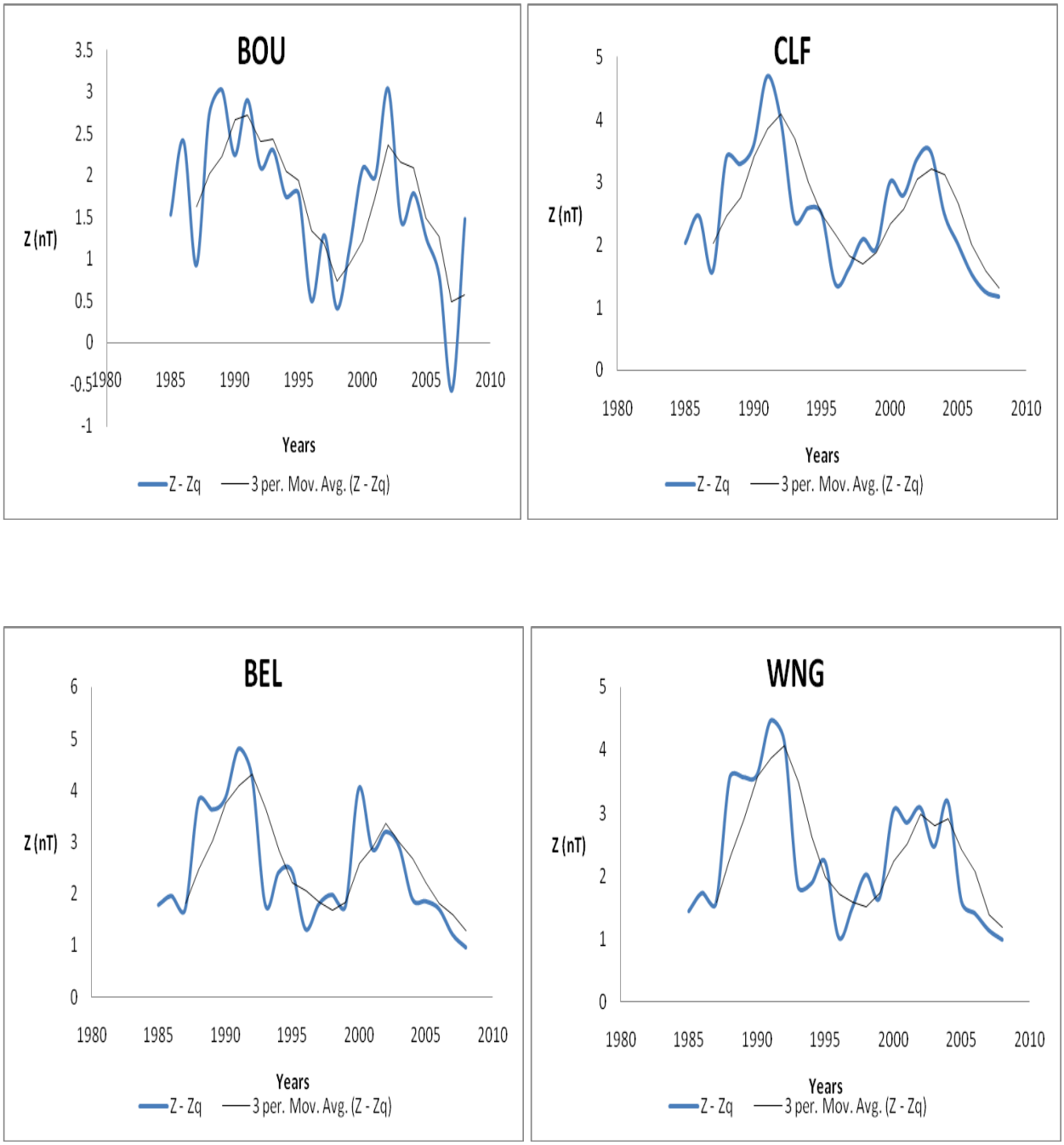

Figure 3.8 Z_{diff} for geomagnetic mid latitude stations

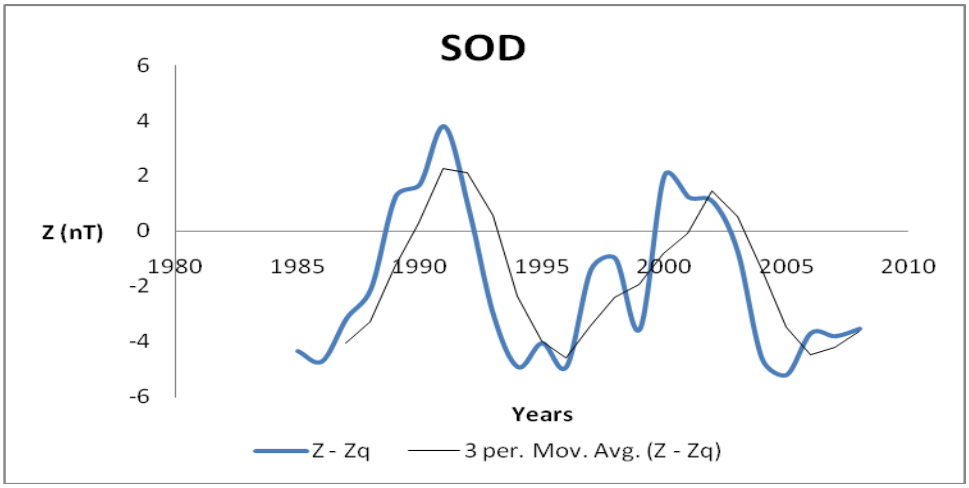

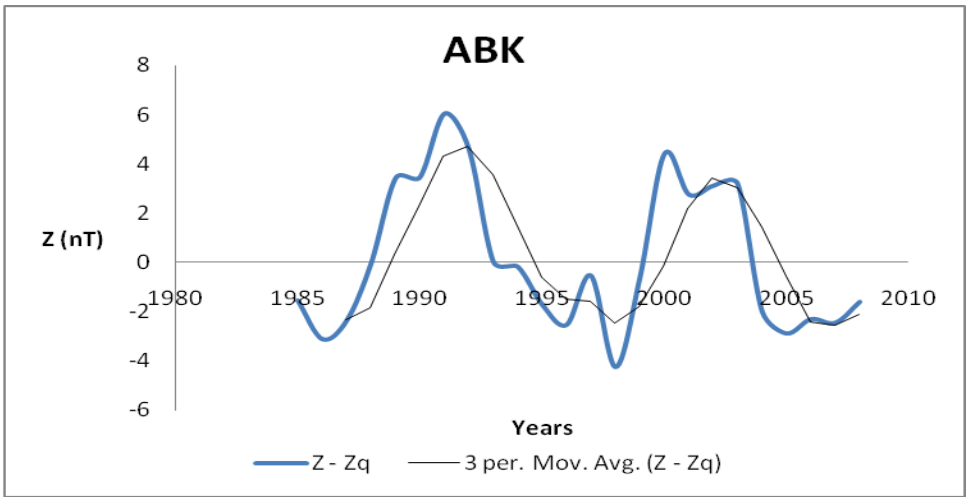

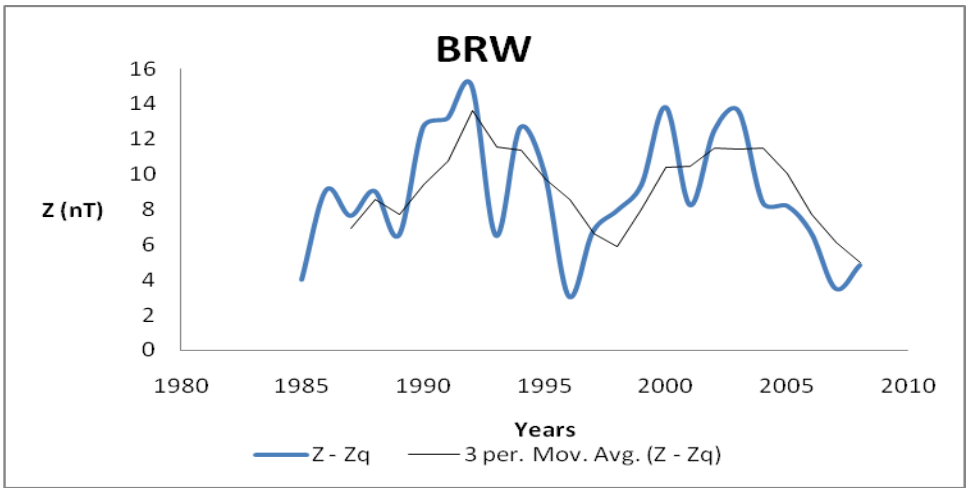

Figure 3.9 Z_{diff} for geomagnetic high latitude stations

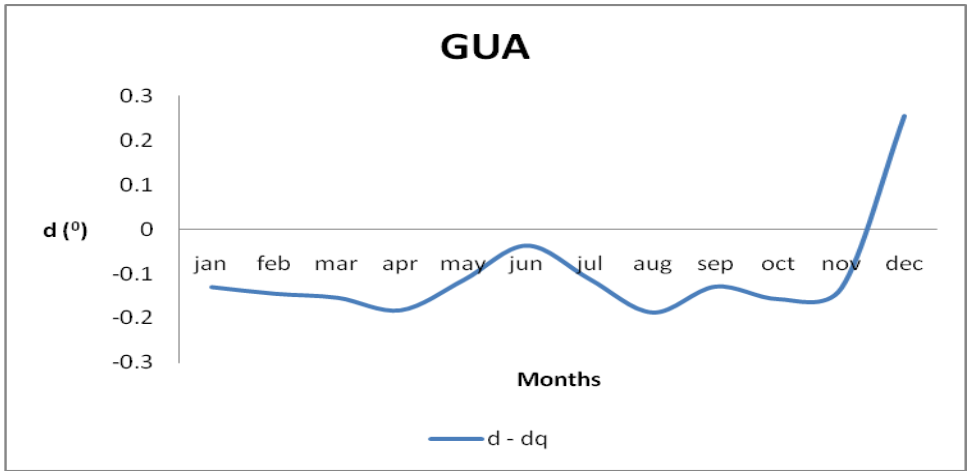

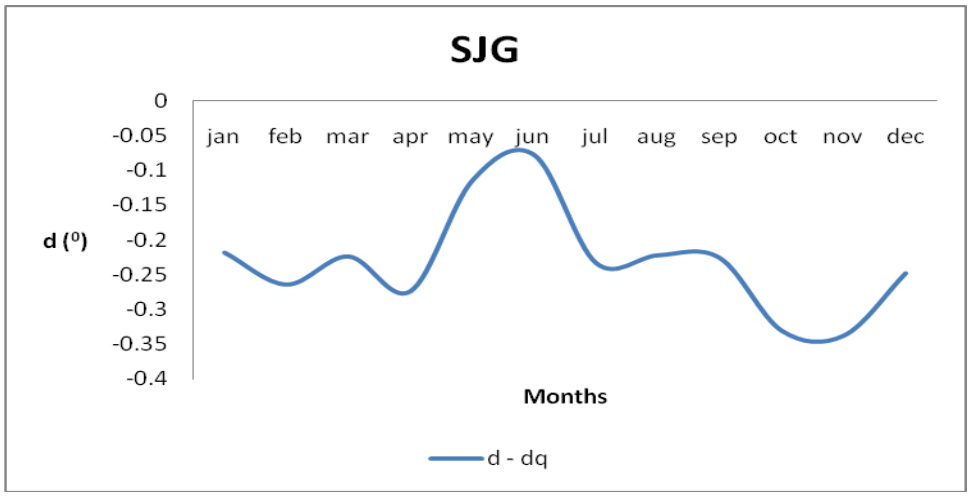

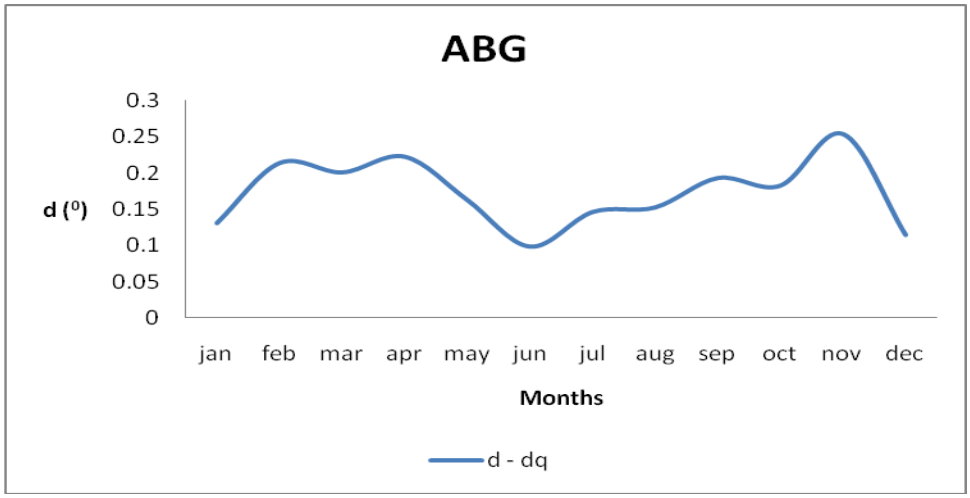

Figure 3.10 d_{diff} for geomagnetic low latitude stations

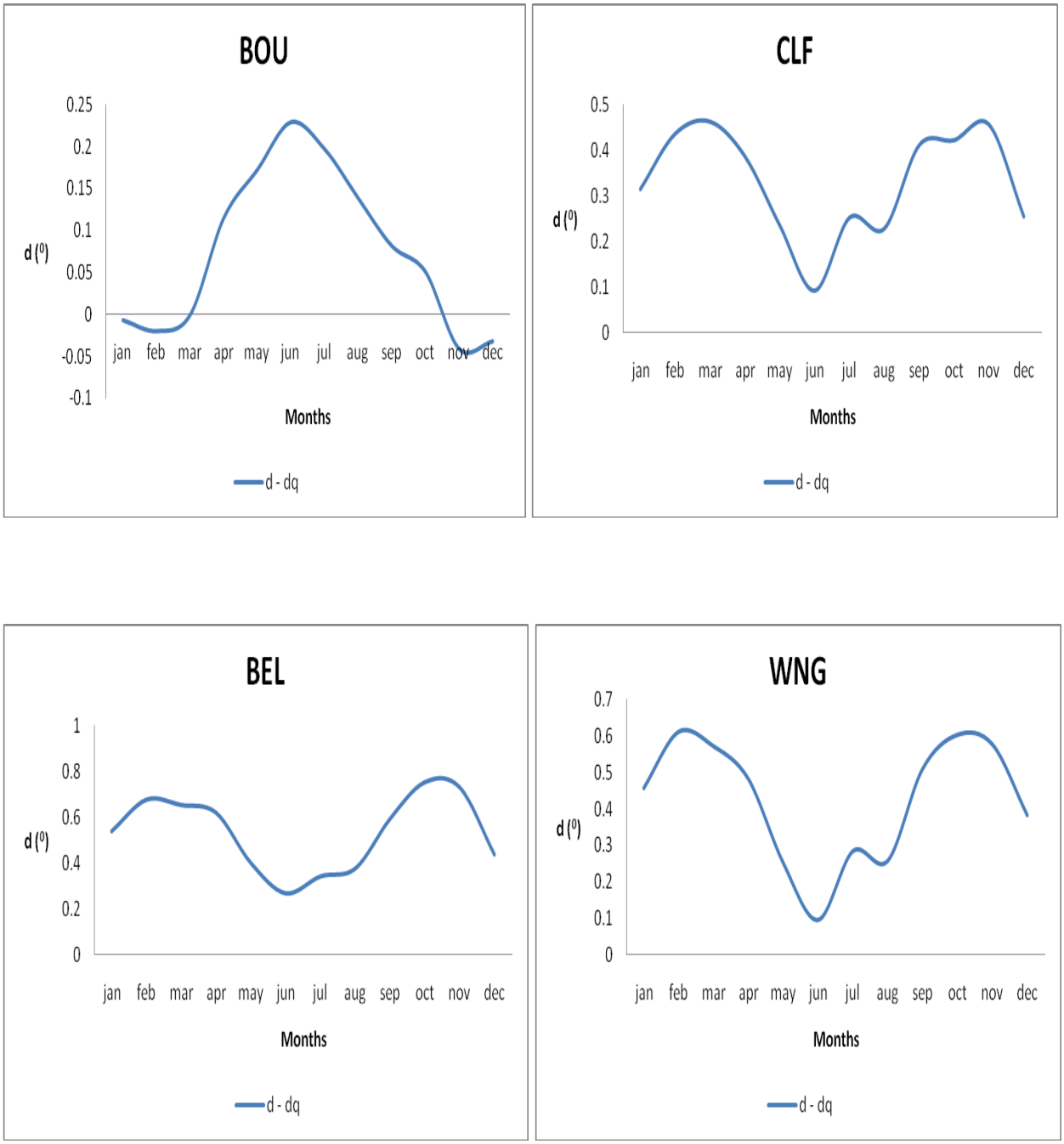

Figure 3.11 d_{diff} for geomagnetic mid latitude stations

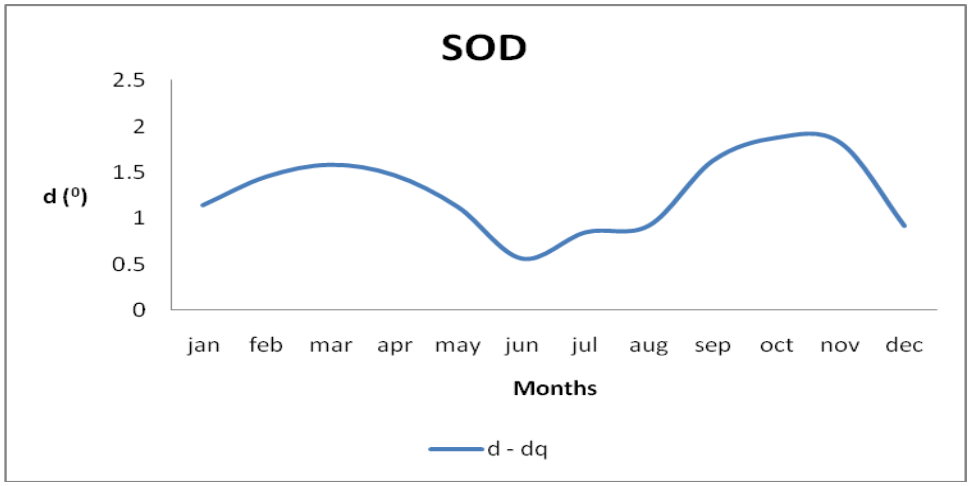

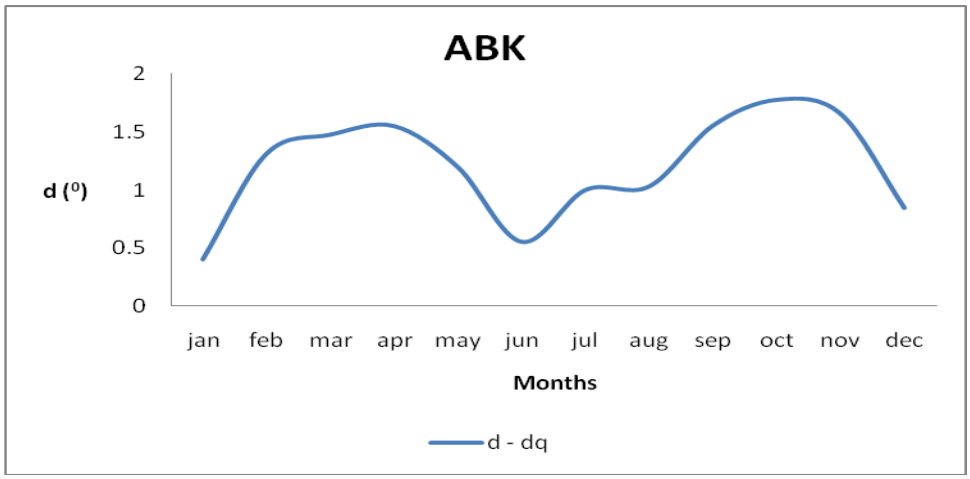

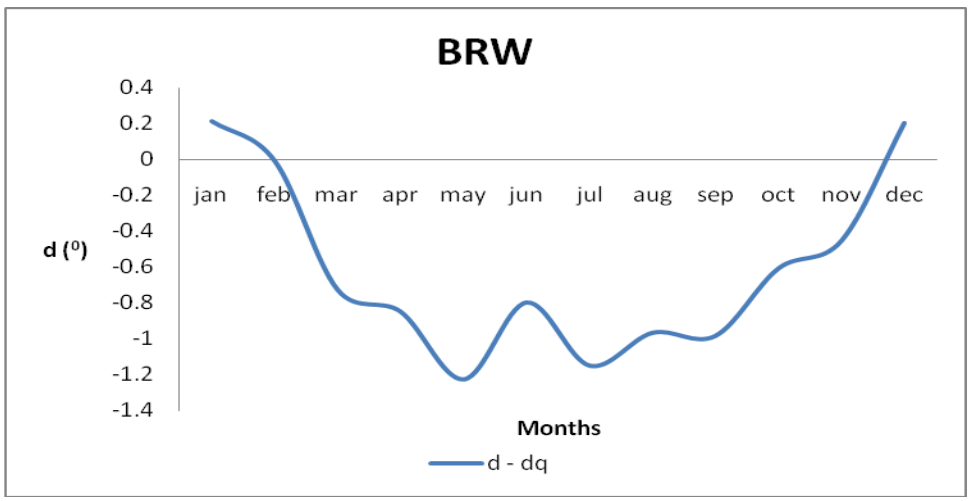

Figure 3.12 d_{diff} for geomagnetic high latitude stations

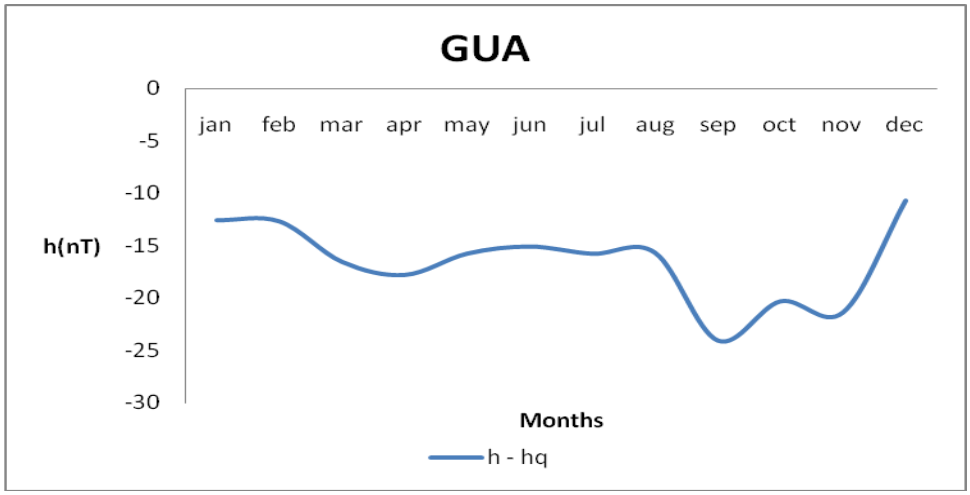

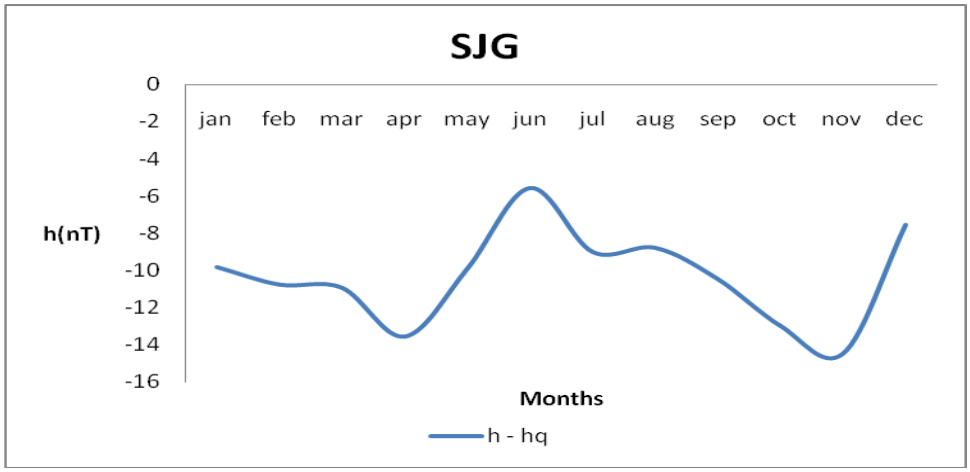

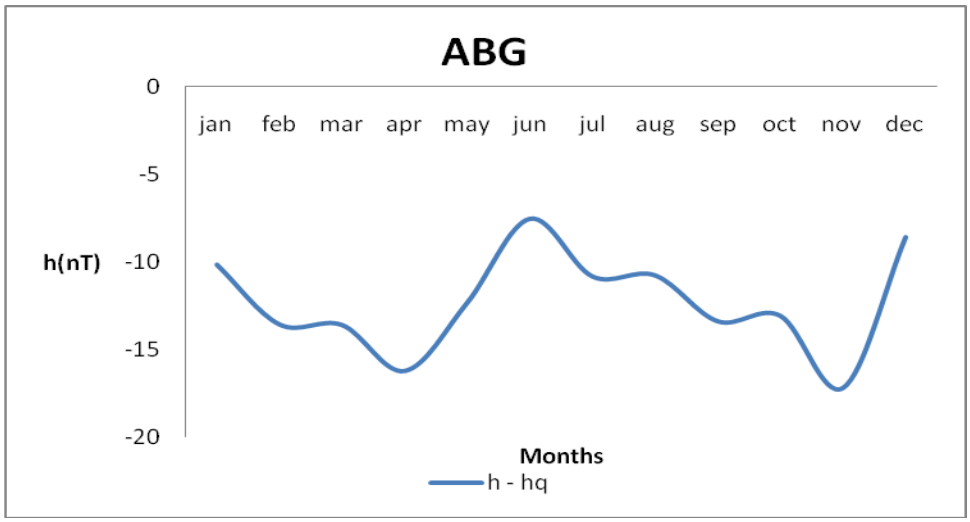

Figure 3.13 h_{diff} for geomagnetic low latitude stations

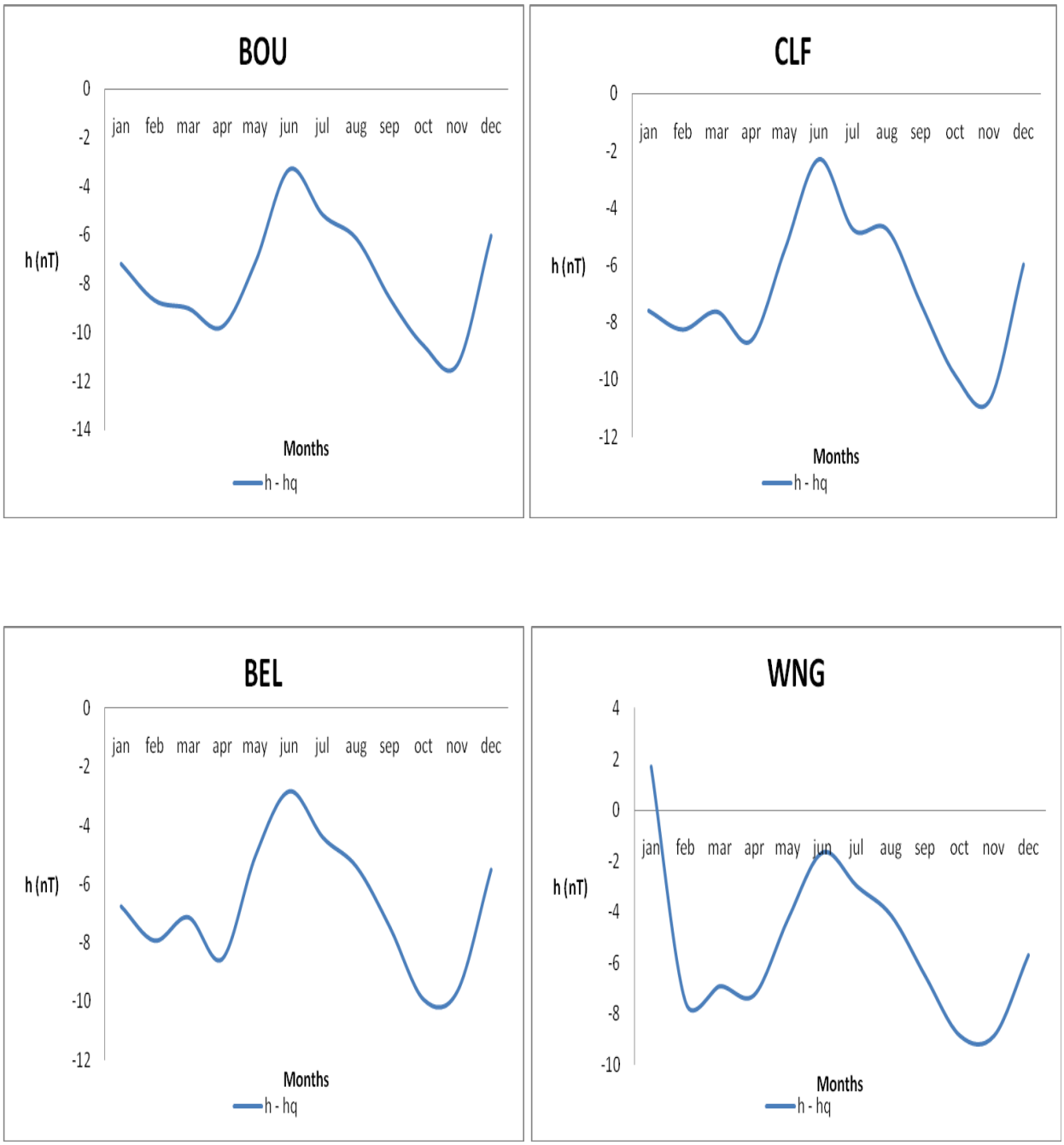

Figure 3.14 h_{diff} for geomagnetic mid latitude stations

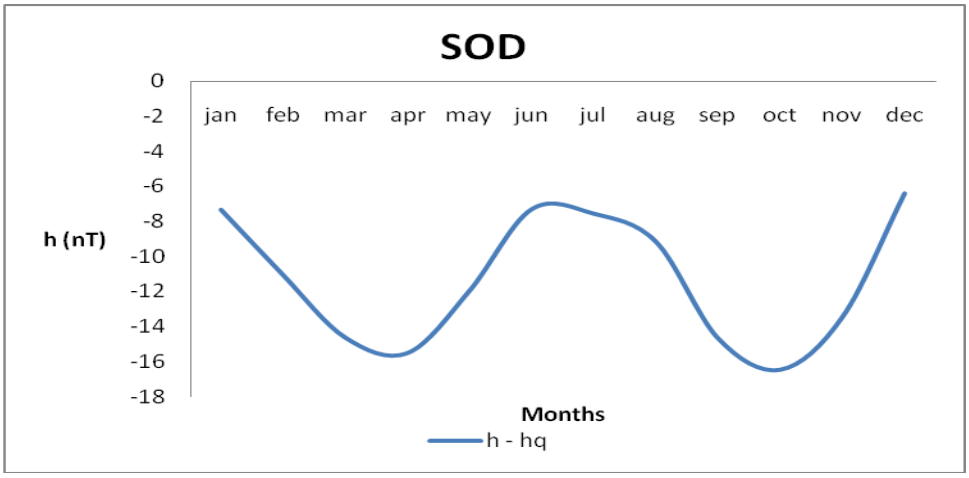

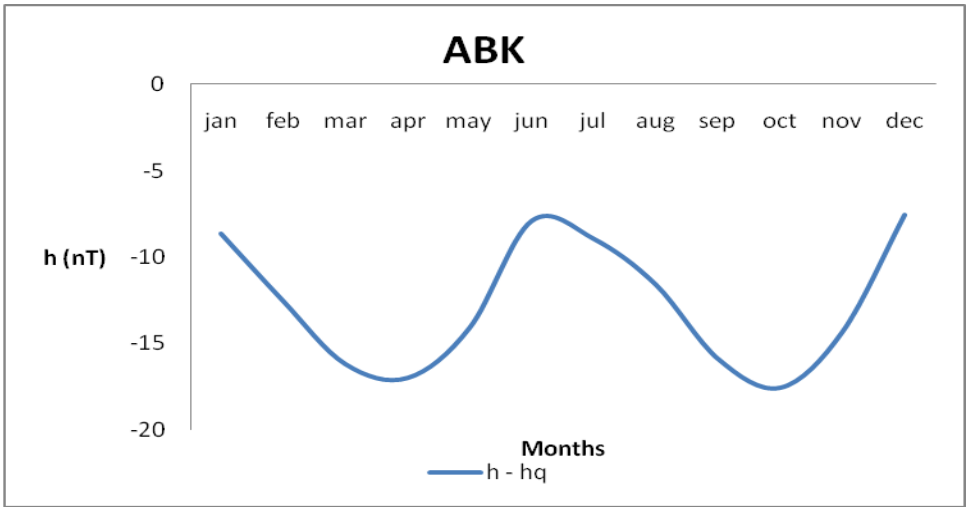

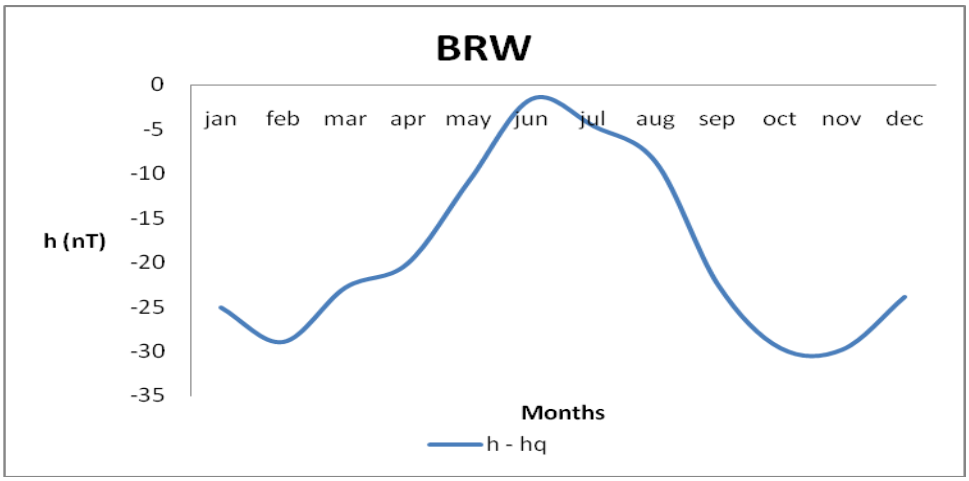

Figure 3.15 h_{diff} for geomagnetic high latitude stations

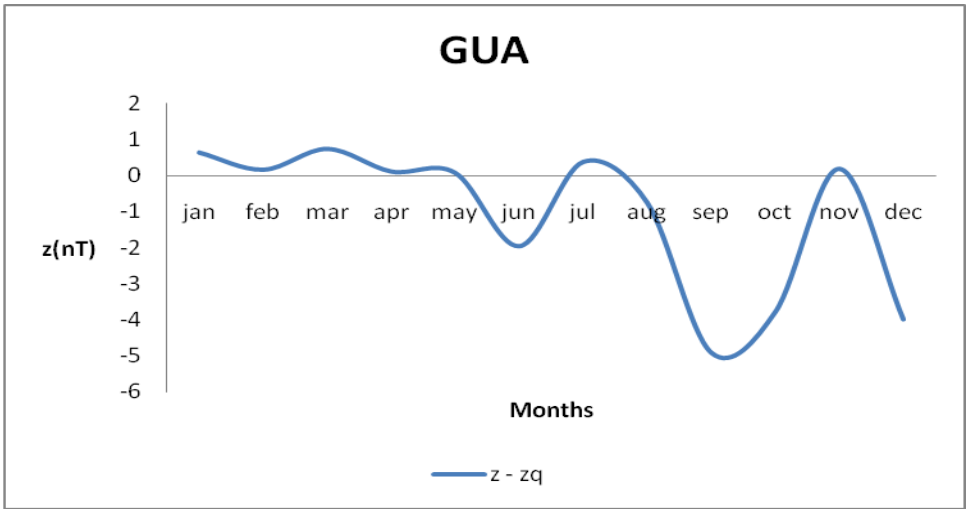

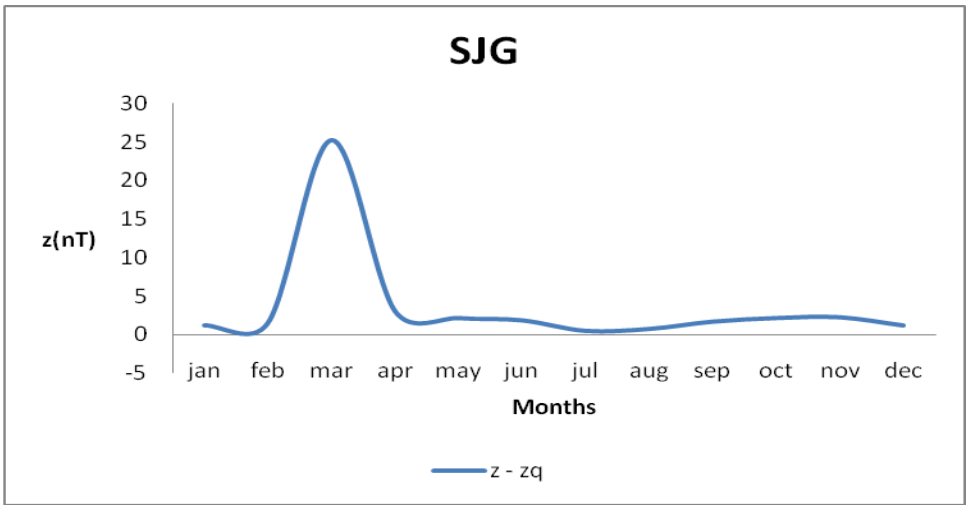

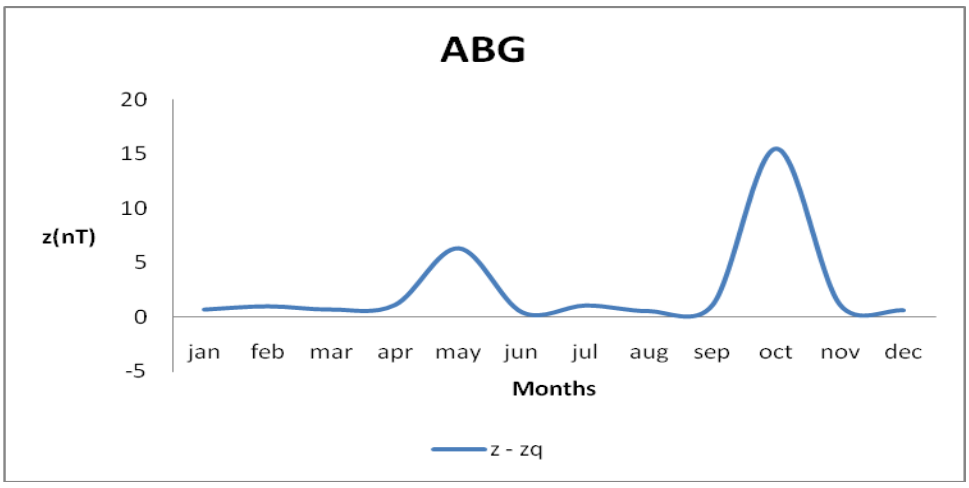

Figure 3.16 z_{diff} for geomagnetic low latitude stations

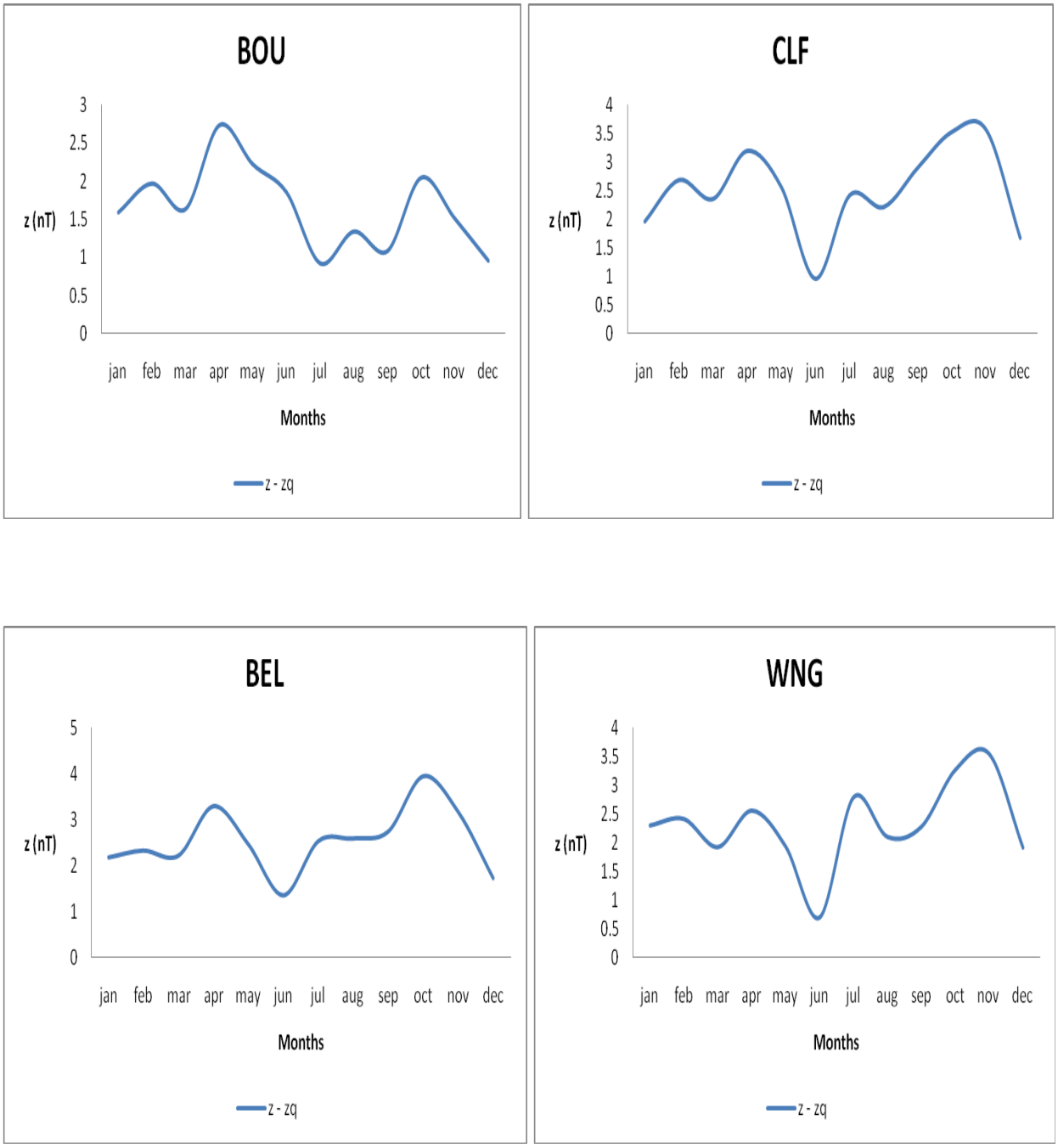

Figure 3.17 z_{diff} for geomagnetic mid latitude stations

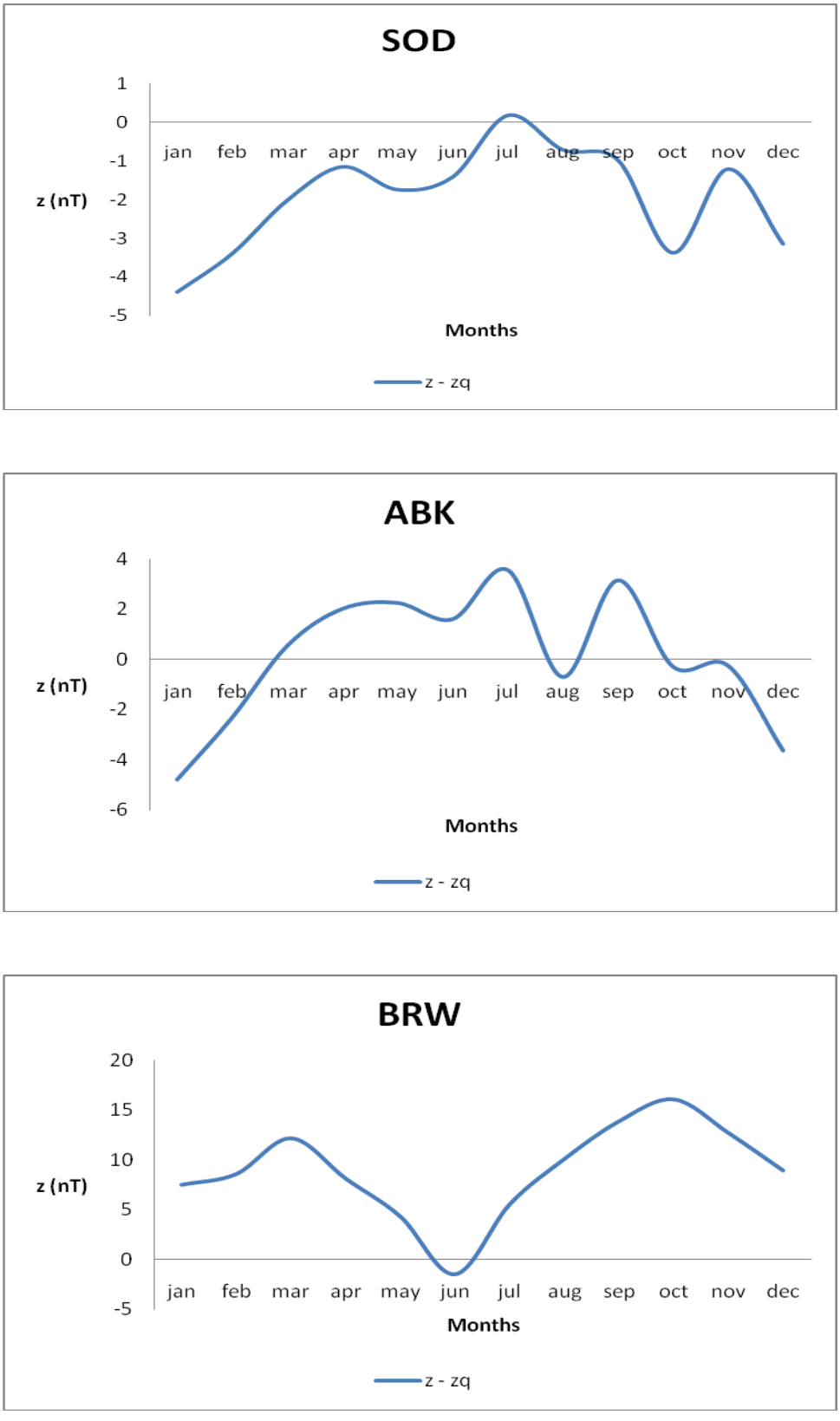

Figure 3.18 z_{diff} for geomagnetic high latitude stations

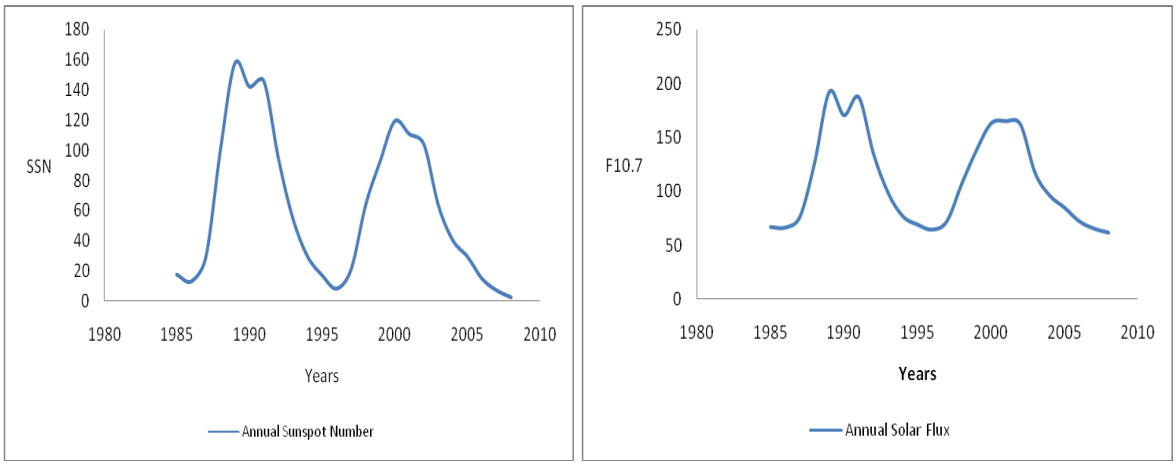

Figure 3.19 annual mean SSN & F10.7 during cycle 22 and 23

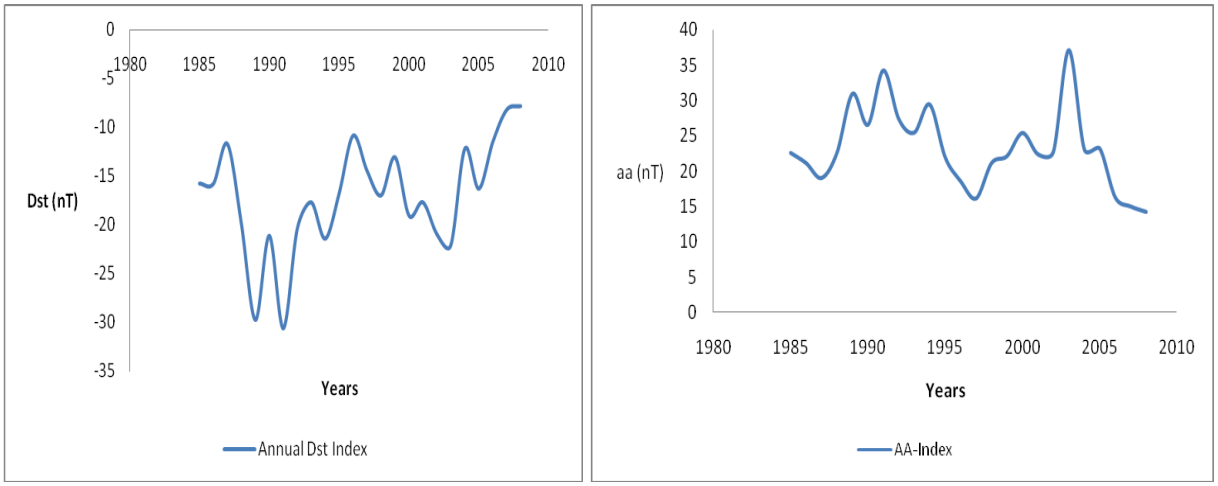

Figure 3.20 Mean annual Dst & aa index during cycle 22 and 23

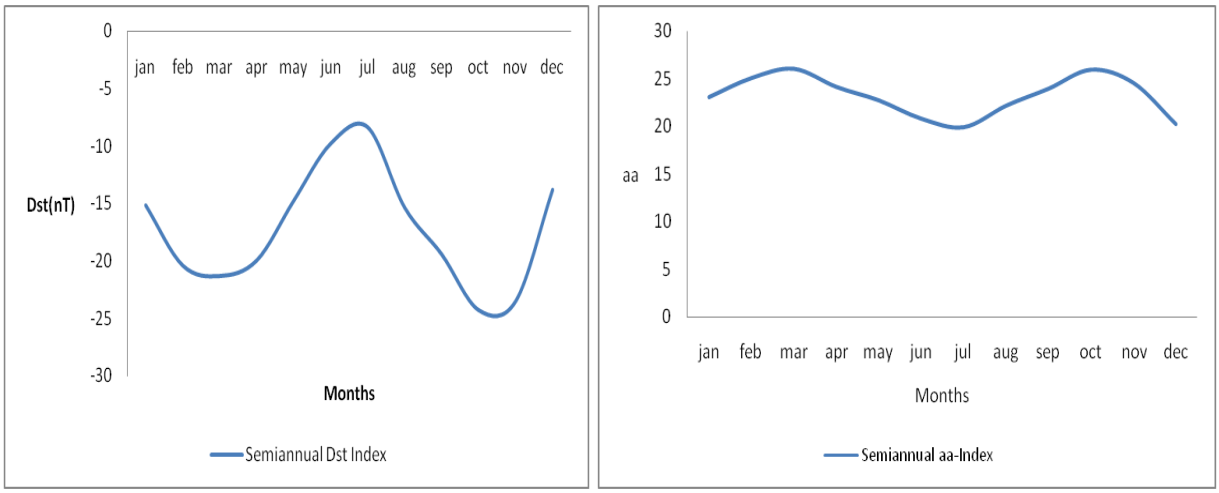

Figure 3.21 semiannual Dst & aa index during cycle 22 and 23

Table 3.2 Correlation coefficients of Sunspot number against the annual components

	D_{diff}	H_{diff}	Z_{diff}
Guam	-0.83	-0.75	-0.33
San Juan	-0.47	-0.74	0.53
Alibag	0.67	-0.74	-0.06
Boulder	0.55	-0.70	0.65
Chambon-la-foret	0.48	-0.76	0.80
Belsk	0.71	-0.74	0.86
Wingst	0.51	-0.75	0.86
Sodankyla	0.13	-0.23	0.87
Abisko	-0.14	0.06	0.82
Barrow	-0.36	0.43	0.57

Table 3.3 Correlation coefficients of Dst against the annual components

	D - Dq	H - Hq	Z – Zq
Guam	0.77	0.82	0.10
San Juan	0.67	0.95	-0.46
Alibag	-0.68	0.89	-0.16
Boulder	-0.64	0.93	-0.74
Chambon-la-foret	-0.75	0.94	-0.88
Belsk	-0.85	0.94	-0.84
Wingst	-0.83	0.93	-0.78
Sodankyla	-0.55	0.64	-0.70
Abisko	-0.31	0.40	-0.75
Barrow	0.47	-0.19	-0.61

Table 3.4 Correlation coefficients of aa-index against the annual components

	D - Dq	H - Hq	Z – Zq
Guam	-0.56	-0.75	0.12
San Juan	-0.69	-0.86	0.46
Alibag	0.55	-0.88	0.25
Boulder	0.47	-0.87	0.56
Chambon-la-foret	0.78	-0.88	0.82
Belsk	0.87	-0.88	0.70
Wingst	0.79	-0.86	0.66
Sodankyla	0.77	-0.84	0.50
Abisko	0.57	-0.63	0.69
Barrow	-0.37	-0.08	0.68

Table 3.5 Correlation coefficients of F10.7 against the annual components

	D – Dq	H - Hq	Z – Zq
Guam	-0.78	-0.76	-0.36
San Juan	-0.51	-0.72	0.53
Alibag	0.60	-0.71	-0.04
Boulder	0.56	-0.67	0.64
Chambon-la-foret	0.47	-0.74	0.79
Belsk	0.69	-0.72	0.83
Wingst	0.48	-0.75	0.83
Sodankyla	0.11	-0.23	0.88
Abisko	-0.16	0.06	0.84
Barrow	-0.36	0.46	0.57

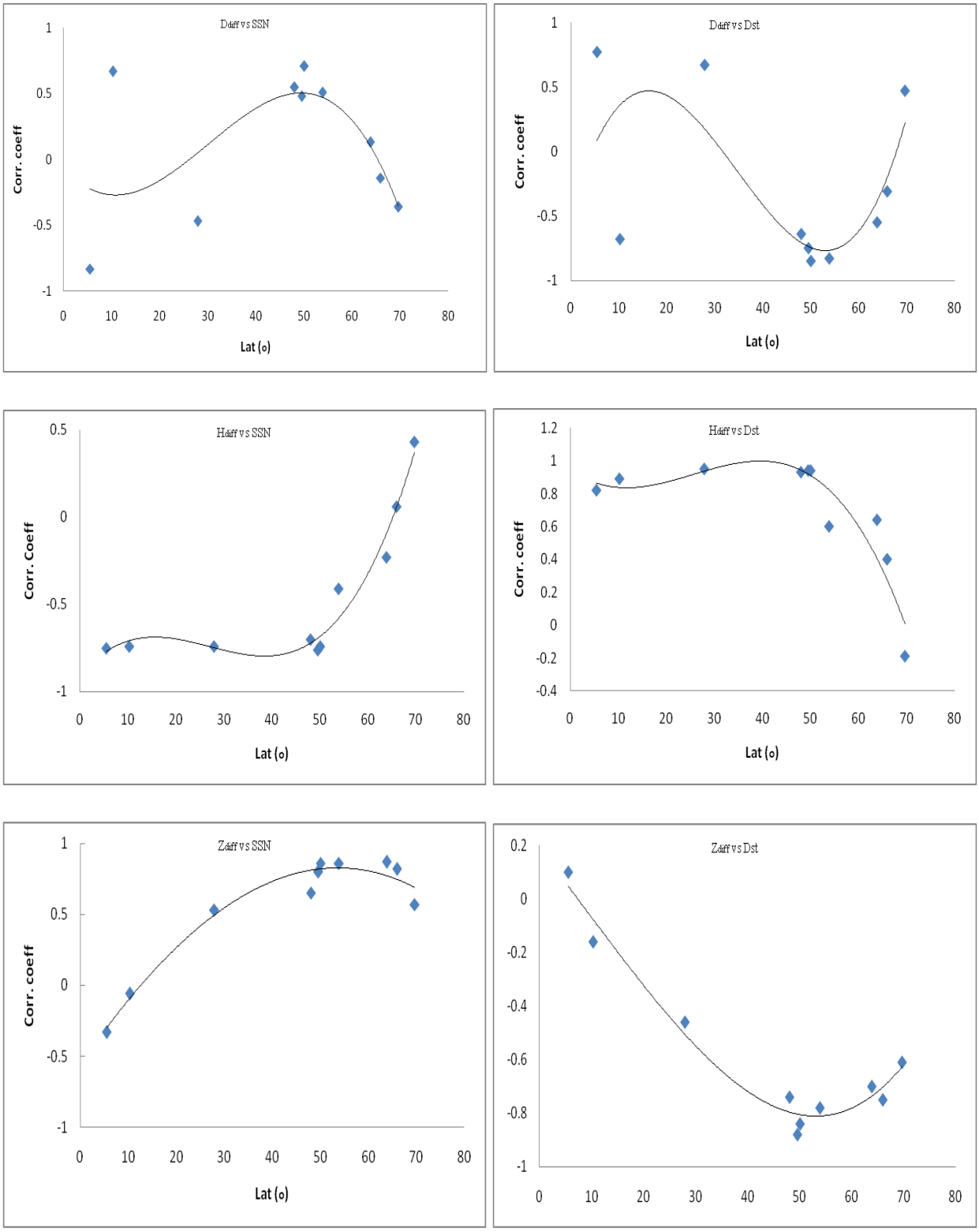

Fig. 3.22 SSN & Dst correlation plots of D_{diff}, H_{diff} and Z_{diff} for all geomagnetic latitudes used in this study

CHAPTER FOUR

DISCUSSION

4.1 D Component Variation

D_{diff} showed a periodic variation which is more evident when the 3-point moving average is superposed on the annual variation. The 3-point moving average showed two clear peaks which suggest a solar activity forcing of the field variation. The solar activity forcing is most observable in the mid-latitudes and weakest in the low and high-latitude stations. This is expected since declination tends to zero in the low-latitude. Only mid latitude stations showed common pattern of Sunspot (SS) cycle

The low latitude stations showed inconsistency from year to year viz-a-viz station to station with no clear resemblance with SS cycle. Mid latitude stations showed common pattern of D_{diff} (positive) peaks during solar maximum and troughs during solar minimum, this pattern follows the SS cycle although out of phase while high latitude stations exhibits strong variability from year to year with no clear resemblance with SSN and F10.7 (figure 3.1, 3.2 & 3.3). The latitudinal distribution of the correlation (at 95% confidence) for the 10 stations is presented in figure 3.22; we observed a clear latitudinal profile of the association between D_{diff} and the SSN, and also between D_{diff} and Dst.

The D_{diff} showed good correlation with Sunspot Number for mid latitude stations, good but negative in low latitude stations, very weak and negative in high latitude stations. A similar correlation with F10.7 was observed. D_{diff} correlation with Dst-index was good in low and mid latitude stations and becomes weak in high latitude stations; the correlation was positive for low latitude then become negative for mid and high latitude. D_{diff} correlated well with aa-index in all geomagnetic latitude stations except for Barrow with 0.4

The semi- annual variation of d_{diff} (figure 3.10, 3.11 & 3.12) showed clear seasonal effects with peaks for middle and high latitude stations during April (spring) and Oct-Nov (fall) except for BOU and BRW. Low latitude stations showed no seasonal variations.

4.2 H Component Variation

The H_{diff} showed a periodic vibration especially for low and mid latitude geomagnetic stations which is more evident when the 3-point moving average is superposed on the annual variation. The low geomagnetic latitude stations GUA, SJN, ABG showed clear annual H_{diff} (figure 3.4) which closely follow the 11-year sunspot cycle. H_{diff} exhibited a negative peak which is expected since the geomagnetic H-component during quiet conditions will be stronger than the field during more disturbed conditions. In mid-latitude geomagnetic stations (figure 3.5), a similar trend is observed but with a smaller peak generally less than -12nT. For high latitude stations, H_{diff} annual means tend to be highly variable from year to year with no clear semblance with the 11 year sunspot (SS) cycle. All stations within the same latitude group (i.e. for low and mid latitude groups) showed common pattern of H_{diff} peaks during solar maximum and troughs during solar minimum. The trend is generally not in phase with the SS cycle but closely follows the variation of the mean annual Dst (figure 3.20). This suggests that the magnetospheric response to the solar wind modulation of its field is not always in phase with the process of the sun (Verbanac, et al., 2006). The latitudinal distribution of the correlation (at 95% confidence) between H_{diff} and SSN, Hdiff and Dst for the 10 stations is presented in figure 3.22; there is a clear latitudinal profile of the association between H_{diff} and the SSN. The H_{diff} for the 24 years used in this study correlated well (>0.5) with the SSN for low and mid latitudes stations. The association between the H_{diff} and SSN becomes weaker and positive in higher latitudes stations. The correlation with Dst was good for low and mid latitude stations and becomes weaker and negative in high latitude stations. The H_{diff} showed good correlation with aa-index across the latitudes except for Barrow with 0.08. The correlation between the H_{diff} and F10.7 was good for low latitude & mid latitude stations, and then it becomes weaker and positive in higher latitudes stations.

The semi- annual variation of h_{diff} (figure 3.13, 3.14 & 3.15) showed clear seasonal effects with negative peaks at all latitudes during April (spring) and Oct-Nov (fall). This suggests that the trend is a global natural effect rather than a mere measurement error. Unlike the annual variation which showed latitudinal dependence, the semi-annual hdiff showed no longitudinal or latitudinal dependence. The peaks of the semi-annual variation tend to be slightly greater in the October-November peaks when compared with the April peak. This observation is not trivial by

any means since the Dst semiannual profile (figure 3.21) also exhibited similar trend (i.e. having slightly higher peak in the fall season) and thus confirms the RM hypothesis. Since Dst is a measure of the severity of global magnetic disturbances and the strength of the magnetic field created by the ring current, the North-South migration of this current is the most plausible cause of the seasonality in h_{diff} not only in the low latitudes but in all latitudes in the Northern hemisphere. The semiannual peaks detected in the hdiff for mid and high latitude stations gives credence to result of works by Wardinski and Mandea (2006). It is important to note that the slightly greater peaks in the Oct-Nov months were observed in all the stations used in this study which further supports RM hypothesis.

4.3 Z Component Variation

The Z_{diff} showed a periodic vibration which is more evident when the 3-point moving average is superposed on the annual variation. The Z_{diff} component annual variations for low, mid and high latitude stations are presented in figure 3.7, 3.8 & 3.9 respectively. The mid and high latitude stations show annual variation which follow the pattern of the SS cycle albeit out of phase. Nonetheless, a similar trend in all the stations in a given latitude range suggests common underlying processes leading to the variability. Enhanced values of this parameter were observed during the solar maximum and diminished values during solar minimum. It is interesting to note that the change in Z_{diff} within a solar cycle is generally smaller in the mid latitude and becomes much larger in the high latitude. The low latitude stations exhibited strong variability from year to year with no clear phonological resemblance with the SSN except for SJN station. This observation is corroborated in the correlation analysis in which Z_{diff} correlation with SSN was weak and negative in the low latitude stations and becomes stronger and positive in mid and high latitude stations while the correlation with Dst was weak in low latitude stations and becomes stronger and negative in mid and high latitude stations. This observation in the annual profile of Zdiff is clearly in line with the expectations of the RM hypothesis. The correlation of zdiff with aa-index was weak in low latitude stations, stronger in mid and high latitude stations while the correlation with F10.7 was weak and negative in low latitude stations and becomes stronger and positive in mid and high latitude stations.

The z_{diff} variation did not show similar pattern in the entire stations used (figure 3.16, 3.17 and 3.18). The seasonal effect was not evident and its variability is likely dominated by other localized currents.

CHAPTER FIVE

CONCLUSIONS AND RECOMMENDATIONS

5.1 Conclusions

We have used the effects of ring current on three components of the geomagnetic field to decipher the validity of the Russell-McPherron (RM) hypothesis. We have successfully employed for the first time, the difference in the field strength for all days and Sq days in the month/year and indentified both annual and semiannual variation in the geomagnetic activity. We observed that D_{diff} showed common pattern for mid latitude stations with peaks during solar maximum and troughs during solar minimum, this pattern follows the SS cycle although out of phase. H_{diff} showed annual variation corresponding with the 11year solar cycle especially in low and mid geomagnetic latitudes which was not in phase with the sunspot number (SSN). The Z_{diff} parameter exhibited annual variation which corresponded also with the 11 year solar cycle in the mid and high latitudes and was not in phase with the SSN. The D_{diff} showed strong correlation with Sunspot Number and Dst for mid latitude stations than other latitudes. Strong inverse correlation between H_{diff} and SSN was found at low and mid -geomagnetic latitudes and weaker correlation at high latitudes. Association between Z_{diff} and SSN was stronger at high geomagnetic latitudes than low geomagnetic latitudes while its correlation with Dst was weak in low latitude stations and becomes stronger and negative in mid and high latitude stations. The semiannual variation of d_{diff} and h_{diff} revealed clear semi-annual trend with peaks in April and Oct-Nov. which was similar to the Dst semiannual variation for the same period. This semiannual trend was observed in all stations irrespective of location suggesting a global process such as the North- South migration of the ring current as the underlying dominant process causing this seasonality, and hence validating the RM hypothesis. Figure 3.22 shows a brief latitudinal profile of the association between solar activity and the geomagnetic field strength

5.2 Recommendations

We suggest that future works should be done to cover more solar cycles. The scope should also include stations in the southern hemisphere

REFERENCES

Balan, N., Y. Otsuka, G. J. Bailey, S. Fukao, and M. A. Abdu, (2000) Annual variations of the ionosphere: A review based on the MU radar observations, *Adv. Space Res.*, **25**, 153–162.

Bartels, J. (1932) Terrestrial-Magnetic activity and its relation to solar phenomena; Terrestrial magnetic and Atmospheric Electricity, 37, 1

Bhardwarj S. K. Subba Rao P.B.V (2013) Secular trend of geomagnetic elements in the Indian region; Earths Planet Space, **65**, 1515-1523

Bolton, S. (1990) One year variation in the near earth solar wind ion density and bulk flow velocity, *Geophys. Res. Lett.*, **17**, 37–40

Chulliat A. Blanter E., Le Mou¨el J.-L., Shnirman (2005), on the seasonal asymmetry of the diurnal and semidiurnal geomagnetic variations, Journal of Geophys. Res. 110, A05301

Cliver E.W. Kamide Y. Ling A.G. (2002) The semiannual variation of geomagnetic activity phase and profiles for 130 years of aa data. Journal of atmospheric and solar terrestrial Physics **64**, 47-53

Courtillot, V. and J.-L Le Mou¨el (1988) Time variations of the Earth's magnetic field: from daily to secular, *Ann. Rev. Earth Planet. Sci*, **16**, 389–476.

Gonzalez, W. D., J. A. Joselyn, Y. Kamide, H. W. Kroehl, G. Rostoker, B. T. Tsurutani, and V. M. Vasyliunas (1994), What is a Geomagnetic Storm?, J. Geophys. Res., 99(A4), 5771–5792

Joe Buchdahl. "Atmosphere, Climate & Environment Information Programme". Ace.mmu.ac.uk. Retrieved 2012-04-18

Kopp, G., Lawrence, G. and Rottman, G. (2005) "The Total Irradiance Monitor (TIM): Science Results". *Solar Physics* **20** (1–2): 129–139

K. Rawer. *Wave Propagation in the Ionosphere*. Kluwer Acad.Publ., Dordrecht (1993). ISBN 0-7923-0775-5

Le Mou¨el J.-L., E. Blanter, A. Chulliat, and M. Shnirman, (2004) On the semiannual and annual variations of geomagnetic activity and components, *Ann. Geophys.*, **22**, 3583–3588.

Malin, S. R. C. and A. M. Isikara, (1976) Annual variation of the geomagnetic field, *Geophys. J. R. astr. Soc.*, **47**, 445–457

Malin, S. R. C. and D. E. Winch, (1996) Annual variation of the geomagnetic field, *Geophys. J. Int.*, **124**, 170–174.

Malin, S. R. C., D. E. Winch, and A. M. Isikara, (1999) Semi-annual variation of the geomagnetic field, *Earth Planets Space*, **51**, 321–328.

McGraw-Hill Concise Encyclopedia of Science & Technology, (1984) Troposhere "It contains about four-fifths of the mass of the whole atmosphere."

McIntosh, D. H. (1959), On the annual variation of magnetic disturbance, Philosophical Transactions of the Royal Society of London, Series A, 251, 525

Menzel, Whipple, and de Vaucouleurs, (1970) "Survey of the Universe"

Mursular K., Tanskaners E., and Love J.J. (2011) Spring-fall asymmetry of substorm strength, geomagnetic activity and solar wind: Implications for semiannual variation and solar hemispheric asymmetry. Geophysical Research letters, 38, L06104

NASA Science News, "Polar Substorm", 2009-03-02. http://science.nasa.gov/science-news/science-at-nasa/2000/ast02mar_1m/. Retrieved 2013-12-28

Nicky Fox, "Coronal Mass Ejections". Goddard Space Flight Center @ NASA. Retrieved 2011-04-06

Okeke F. N. and Y. Hamano, (2000) Daily variations of geomagnetic *HD* and *Z*-field at equatorial latitudes, *Earth Planets Space*, **52**, 237–243.

Rao and Bansal (1969), Secular variation of geomagnetic elements at Alibag, Indian Journal of Meteorology and Geophys., **20**, 141-144

Rastogi R.G. Alex S. Patil A. (1994), Seasonal variation of the geomagnetic D,H, Z fields at low latitudes, Journal of Geomag. Geolec. **46**, 115

Russell, C. T. and R. L. McPherron, (1973) Semiannual variation of geomagnetic activity, *J. Geophys. Res.*, **78**, 92–108.

Silverman, S. M. and R. Shapiro, (1983) Power spectral analysis of auroral occurrence frequency, *J. Geophys. Res.*, **88**, 6310–6316.

States, Robert J.; Gardner, Chester S. (January 2000). "Thermal Structure of the Mesopause Region (80–105 km) at 40°N Latitude. Part I: Seasonal Variations". *Journal of the Atmospheric Sciences 2000* **57**: 66–77

Sugiura, M., and T. Kamei, (1991) Equatorial Dst index 1957-1986, IAGA Bulletin, 40, edited by A. BerthelJer and M. MenvielleI,S GI Publ. Off., Saint. Maur-des-Fosses, France.

Svalgaard L. (1977), Geomagnetic activity: dependence on solar wind parameters, In : Zirker J. B. (E.d), Coronal Holes and High speed wind streams, Colorado Associated Univ. Press, Boulder, 371

Svalgaard L., Cliver E. W., (2007); Inter hourly variability index of geomagnetic activity and its use in deriving the long term variation of solar wind speed, J. Geophysical Res. 112, A10111.

Svalgaard, L., (2011), Geomagnetic semiannual variation is not overestimated and is not an artifact of systematic solar hemispheric asymmetry

Verbanac G. Luhr H., Rother M., (2006), Evidence of the ring current effect in geomagnetic observatories annual means. GEOFIZIKA, 23(1), 13

Wardinski, I., Mandea, M. (2006) Annual and semi-annual variations of the geomagnetic field components analyzed by the multi-taper method. - Earth Planets and Space, **58**, 6, 785- 791.

Yamazaki, Y., Yumoto K. (2012), Long term behaviour of annual and semi-annual Sq variations, Earthplanet Space, **64**, 417.

Zieger, B. and K. Mursula, (1998) Annual variation in near-earth solar wind speed: Evidence for persistent north-south asymmetry related to solar magnetic polarity, *Geophys. Res. Lett.*, **25**, 841–844.

APPENDIX

Table for Annual variation of D for all stations

Year	Alibag	Guam	San juan	Belsk	CLF	Wingst	Boulder	Abisko	Sodankyla	Barrow
1985	-13.7485	12.79484	66.56415	-48.4174	-86.6338	-74.1712	62.18943	-83.9776	-73.9448291	165.1345
1986	-11.6995	12.28871	59.45097	-44.3032	-79.3716	-67.599	57.9697	-78.3151	-68.7068325	159.4364
1987	-10.296	11.62314	52.30657	-41.0396	-71.8386	-61.7389	53.51938	-73.0865	-64.4802968	154.5342
1988	-8.80799	10.00263	44.94729	-37.3073	-64.5182	-55.6386	49.57087	-67.2365	-59.1817336	146.0748
1989	-7.22954	9.231792	37.35496	-33.9666	-57.2762	-49.5978	45.80733	-61.2612	-53.8551399	138.2705
1990	-6.02153	8.309366	29.96752	-31.2261	-50.9616	-44.5785	41.96846	-57.8641	-50.394451	128.6336
1991	-4.65042	7.245963	22.27267	-27.9588	-44.3629	-39.1745	38.69221	-52.0682	-45.5893972	120.1172
1992	-3.97091	6.387352	15.2089	-25.0209	-38.2472	-34.0648	35.04954	-46.7536	-41.3961919	109.456
1993	-2.94821	5.26658	8.296895	-20.7509	-31.2103	-27.7116	31.60057	-39.5905	-34.6993767	97.76321
1994	-2.55096	4.443264	1.464041	-15.9366	-23.5868	-20.6637	27.78038	-30.248	-26.355557	84.55919
1995	-2.43767	3.294928	-4.28999	-11.0544	-9.34267	-13.6821	23.06631	-22.3998	-19.6701423	66.70412
1996	-1.02176	2.132735	-9.70774	-6.07347	-1.78577	-6.29279	16.79599	-13.4497	-11.7836299	45.42422
1997	0.661934	0.813126	-15.3511	-0.46496	0.357406	1.729257	11.39928	-3.50644	-2.6975333	26.10017
1998	1.405011	-0.65219	-21.0182	5.669342	14.47981	9.819034	4.181377	7.047817	6.7855409	5.99425
1999	1.520128	-1.96486	-26.6519	10.62161	22.00299	16.9501	-2.50327	16.90172	15.2867693	-14.2106
2000	2.4146	-3.27625	-32.0001	15.67414	29.44658	24.02588	-9.68583	26.97187	23.9584813	-36.8982
2001	2.93286	-3.9907	-36.3089	20.56577	36.599	30.81477	-17.1868	36.87856	32.3803018	-59.2113
2002	3.600136	-4.68393	-40.1124	25.73432	43.8483	37.76215	-24.679	47.49509	41.7344984	-82.4667
2003	5.130981	-5.88582	-44.1263	31.31111	51.59824	45.72446	-32.3753	59.99814	52.7924523	-106.286
2004	7.743613	-11.1034	-14.7617	36.24619	58.47391	51.87512	-68.0331	68.6385	59.884321	-184.8
2005	8.6957	-12.5739	-18.8175	41.31782	65.41566	58.85441	-75.3367	77.63751	67.8421353	-206.882
2006	11.2482	-14.2498	-22.208	46.15979	71.8801	65.13794	-82.4958	85.94592	75.1177	-228.511
2007	13.52571	-16.4906	-25.1774	51.90895	78.8023	72.31322	-89.9169	95.84517	83.809841	-251.094
2008	16.50509	-18.9629	-27.3054	58.31127	86.22541	79.90697	-97.3778	106.397	93.1630756	-277.852

*Annual mean were calculated from monthly mean while monthly mean were computed from hourly data obtained from the Observatories

Table for Annual variation of H for all stations

Year	Alibag	Guam	San juan	Belsk	CLF	Wingst	Boulder	Abisko	Sodankyla	Barrow
1985	-10.9849	38.08204	125.079	41.12611	-79.9736	8.63638	218.9856	151.6312	168.8351	282.6515
1986	-35.481	49.41843	113.7756	28.98791	-70.7225	0.03058	202.4104	124.1328	140.8793	255.8982
1987	-43.9084	67.75914	112.9413	24.89203	-69.2694	-2.11038	191.2662	111.6236	123.2762	229.4231
1988	-70.8307	40.17411	97.47636	8.57666	-72.3579	-14.962	163.4466	84.47798	96.33449	196.0879
1989	-97.7113	34.93943	80.0258	-8.20044	-79.3228	-29.1282	131.207	58.85777	65.52523	164.101
1990	-107.114	47.16132	79.63927	-12.8614	-71.9299	-30.538	111.9042	44.63262	50.95999	133.6146
1991	13.19339	40.74274	69.20271	-23.5984	-73.3149	-38.601	82.82885	27.16254	28.50627	101.0388
1992	24.9632	54.09593	76.4238	-19.646	-59.8824	-33.0599	68.44943	17.02572	21.95388	74.12768
1993	31.52383	58.90475	78.6619	-17.9884	-46.2482	-26.825	51.8314	2.28293	9.41634	43.1686
1994	16.0792	49.69248	67.62877	-20.7785	-38.6276	-26.1152	28.40001	-16.0794	-10.472	7.810756
1995	18.39998	57.5881	63.95708	-15.2015	-21.854	-17.7197	9.77524	-14.9321	-10.1861	-2.33972
1996	23.62216	61.50848	56.37923	-8.84364	-4.85776	-8.6782	-13.3398	-19.3678	-15.895	-16.6247
1997	21.86986	48.9036	30.72772	-11.8641	1.45813	-7.73243	-24.9102	-26.1947	-25.1642	-33.0422
1998	11.18413	21.46352	-2.07903	-19.0829	3.75166	-12.1501	-44.2912	-39.5884	-40.9741	-56.2996
1999	16.21835	-5.16834	-24.6027	-17.1247	13.68176	-8.14267	-59.7741	-42.6249	-45.7232	-74.2799
2000	9.64274	-21.4352	-53.1217	-18.6961	19.2187	-6.72874	-78.6735	-45.6888	-51.0887	-83.5417
2001	20.03272	-32.8567	-68.7175	-11.7434	34.49026	3.6297	-87.5268	-45.0238	-50.9941	-93.3361
2002	40.09961	-52.9178	-87.0566	-5.09174	47.3483	12.52898	-98.1329	-46.4619	-53.7938	-105.702
2003	-7.70188	-79.4284	-116.16	-3.97443	51.28208	12.51952	-117.928	-62.7204	-71.3623	-139.048
2004	11.79232	-82.3108	-121.043	5.62892	68.82631	22.12496	-125.464	-55.6868	-65.1383	-141.574
2005	18.73437	-95.0479	-136.78	10.09618	80.65596	29.39568	-139.949	-58.0314	-67.8491	-155.865
2006	33.12322	-95.4787	-140.126	22.52766	103.6628	45.08518	-145.072	-51.2284	-63.9298	-164.691
2007	30.551	-105.592	-148.299	33.24446	122.8458	58.82873	-157.257	-49.4282	-65.0327	-204.939
2008	32.72988	-100.085	-153.907	39.73445	141.1169	69.70578	-168.075	-48.861	-68.0835	-216.634

Table for Annual variation of Z for all stations

Year	Alibag	Guam	San juan	Belsk	CLF	Wingst	Boulder	Abisko	Sodankyla	Barrow
1985	-481.079	-341.064	1743.86	-330.261	-253.333	-307.07	892.0338	-226.801	-237.71502	-66.7172
1986	-430.826	-329.23	1595.765	-302.029	-235.603	-283.213	829.0347	-222.073	-230.13057	-84.482
1987	-413.737	-321.058	1447.029	-279.745	-217.922	-263.106	751.4833	-217.269	-224.34511	-108.013
1988	-403.866	-320.284	1310.159	-245.973	-189.911	-231.229	691.0311	-199.549	-207.0765	-111.393
1989	-391.874	-305.523	1169.671	-210.204	-159.87	-197.33	633.9075	-172.23	-181.86966	-106.808
1990	-388.682	-289.47	1023.358	-188.052	-141.172	-176.283	566.6349	-170.274	-176.9477	-116.388
1991	-288.635	-265.09	878.0317	-162.991	-119.296	-151.439	509.8806	-152.133	-159.97018	-117.337
1992	-286.959	-222.815	722.3894	-146.248	-107.953	-136.56	442.5737	-151.1	-159.64142	-122.028
1993	-273.134	-166.653	562.1483	-128.614	-95.9849	-120.158	372.7579	-142.97	-152.09277	-126.15
1994	-241.024	-104.321	403.9989	-100.042	-76.1777	-94.5632	301.3978	-123.736	-132.2085	-119.314
1995	-202.144	-55.0757	242.8732	-75.5456	-60.6296	-73.417	217.9378	-106.58	-110.51876	-122.583
1996	-143.347	-2.6209	83.80589	-50.4717	-46.0391	-52.7061	128.6256	-87.4808	-89.06713	-126.257
1997	-80.4327	50.96799	-74.4573	-15.2116	-22.0181	-20.6909	40.37476	-54.7198	-53.76248	-104.123
1998	20.0565	109.788	-231.237	24.79155	11.49063	18.28177	-47.0343	-18.1815	-11.27018	-67.4123
1999	34.56287	160.0622	-391.903	58.24294	38.50192	51.23849	-147.9	22.61997	24.74038	-28.1574
2000	92.01223	196.9264	-542.478	96.4033	71.84373	90.91997	-249.888	69.02183	72.696	16.3084
2001	157.9521	217.1527	-699.181	132.5921	99.4608	124.1005	-361.338	106.7374	113.01122	50.17979
2002	230.8976	240.9215	-853.308	171.403	130.531	160.555	-470.124	153.2166	160.13753	100.2051
2003	351.0259	254.9316	-995.607	217.3819	170.6486	204.991	-568.976	205.2465	209.88916	159.6495
2004	445.1105	265.8289	-1153.55	248.4218	195.7332	236.4858	-679.946	233.2392	241.95753	184.6511
2005	535.7185	282.5975	-1311.76	282.3924	223.2966	268.392	-789.704	267.3721	277.6518	217.7811
2006	620.8324	297.8408	-1477.21	305.0002	240.7159	290.2929	-911.013	296.2788	307.88771	234.2385
2007	713.041	314.7656	-1639.93	334.5529	261.781	318.0333	-1021.08	329.9175	342.52276	265.2189
2008	824.6184	331.4135	-1811.39	364.1474	281.8898	344.5488	-1130.69	361.5539	376.12251	298.9234

Table for Annual variation of D_q for all stations

Year	Alibag	Guam	San juan	Belsk	CLF	Wingst	Boulder	Abisko	Sodankyla	Barrow
1985	-13.7814	12.7408	66.51606	-48.3587	-86.5739	-74.1223	62.17777	-84.2995	-74.0004	165.1834
1986	-11.8498	12.27116	59.57268	-44.3533	-79.0556	-67.692	57.93065	-78.4748	-68.8822	159.2732
1987	-10.2932	11.51607	52.19954	-40.8242	-71.696	-61.553	53.56355	-72.6529	-63.9115	154.3298
1988	-8.90351	10.0538	44.93503	-37.4311	-64.4829	-55.662	49.52839	-66.8566	-59.0609	146.2583
1989	-7.44944	9.326789	37.43718	-34.244	-57.5608	-49.9514	45.76586	-61.6589	-54.186	138.0917
1990	-6.23013	8.402015	29.96117	-31.4016	-51.1041	-44.7493	41.92245	-57.8132	-50.5622	128.9677
1991	-4.65119	7.272697	22.38238	-28.1647	-44.4648	-39.2863	38.48093	-51.9093	-45.7742	120.9477
1992	-4.00693	6.443479	15.20671	-25.1208	-38.3131	-34.1367	35.0496	-46.6798	-41.4263	110.337
1993	-2.9046	5.223854	8.23961	-20.7416	-31.2521	-27.7698	31.56215	-39.8483	-34.9841	97.61797
1994	-2.54763	4.380996	1.530254	-16.0481	-23.7449	-20.8688	27.80108	-31.5349	-27.4534	84.13152
1995	-2.36028	3.236947	-4.26029	-10.9808	-9.35866	-13.6818	23.04634	-22.5042	-19.7096	66.87108
1996	-0.92156	2.103129	-9.74967	-5.88965	-1.72705	-6.21726	16.85933	-13.3151	-11.5452	45.4758
1997	0.736809	0.755323	-15.4049	-0.31333	0.383645	1.802126	11.51487	-3.21454	-2.3315	26.12939
1998	1.577711	-0.66447	-21.0676	5.803959	14.54337	9.925523	4.286989	7.361308	6.980218	6.362488
1999	1.559119	-2.02819	-26.6891	10.72704	22.04729	17.04422	-2.54595	17.17276	15.56952	-14.7051
2000	2.432618	-3.25937	-31.8696	15.52397	29.49423	24.07583	-9.71869	27.35514	24.16758	-37.1242
2001	2.945571	-4.0056	-36.2924	20.6225	36.65937	30.92524	-17.197	37.64757	32.87948	-59.2132
2002	3.600476	-4.67457	-39.9933	25.66398	43.80086	37.71976	-24.803	47.71015	41.83977	-81.7483
2003	5.094134	-5.89848	-44.0183	31.07655	51.44426	45.53025	-32.3242	59.04928	51.84053	-106.309
2004	7.790278	-11.1951	-14.6838	36.14627	58.37471	52.02642	-67.9029	68.06987	59.49755	-184.488
2005	8.703138	-12.6505	-18.779	41.3261	65.34774	58.83157	-75.4444	77.20781	67.6875	-206.429
2006	11.32567	-14.3198	-22.3029	46.31737	72.00376	65.30598	-82.4719	86.09085	75.42337	-228.444
2007	13.65199	-16.5759	-25.2652	52.08789	78.84592	72.43782	-89.7322	96.09968	84.19883	-253.394
2008	16.58518	-19.0609	-27.4209	58.57698	86.38092	80.0659	-97.3501	106.9965	93.74312	-278.132

Table for Annual variation of H_q for all stations

Year	Alibag	Guam	San juan	Belsk	CLF	Wingst	Boulder	Abisko	Sodankyla	Barrow
1985	-11.8487	36.67417	124.419	40.62094	-80.344	9.0171	217.5239	152.6597	168.6133	285.214
1986	-34.0318	47.36455	113.9906	29.08639	-77.4325	0.94365	202.5303	128.3952	142.6757	256.8895
1987	-47.6761	62.81299	109.5628	22.67258	-71.6476	-3.54302	188.6547	107.4761	118.385	228.1279
1988	-67.8161	42.29275	100.027	9.84767	-71.1652	-13.2305	164.8746	81.39454	94.62744	195.9508
1989	-90.6605	40.59193	85.27795	-4.56061	-74.6407	-24.7148	135.7722	62.86512	70.59549	161.1254
1990	-102.456	49.19142	83.48985	-10.3439	-69.1662	-27.7335	114.5163	42.59569	50.41668	131.9963
1991	21.28728	49.97421	75.21641	-20.4339	-69.9016	-35.4693	87.36418	27.16664	31.63203	97.4786
1992	29.93958	57.75109	80.35996	-17.0607	-56.6937	-30.1067	71.08392	15.8643	21.79258	72.73896
1993	31.64375	58.73075	79.45157	-18.1033	-45.8968	-25.9909	51.87803	3.80087	10.9503	41.57979
1994	18.99172	52.55427	69.47937	-18.6775	-36.3375	-23.1598	31.03224	-4.86542	-1.18897	17.20572
1995	19.86808	57.43073	64.35617	-14.7119	-21.0241	-16.5486	11.15172	-13.4648	-10.0246	1.739916
1996	19.16704	56.02794	52.27076	-11.5544	-7.3995	-10.3451	-16.2739	-20.815	-18.5594	-16.8049
1997	19.3498	46.07705	29.2012	-13.3286	0.01514	-8.17933	-26.6375	-30.0841	-29.2791	-36.3833
1998	-0.79587	18.25284	-4.20853	-20.1113	2.94423	-12.4651	-45.6396	-40.5602	-42.4292	-56.2799
1999	15.06419	1.19097	-27.726	-18.5365	12.60243	-8.67384	-61.4883	-43.7268	-46.9615	-74.2143
2000	11.97968	-22.7156	-52.5515	-17.9751	20.53561	-5.31734	-78.0902	-49.1909	-52.9486	-87.9918
2001	21.99143	-32.974	-68.5875	-11.3059	35.29448	4.55655	-87.191	-49.4924	-53.7379	-97.592
2002	37.49274	-46.2839	-84.2732	-4.13582	48.96825	14.09581	-98.2628	-48.0075	-54.1236	-112.105
2003	-3.8173	-76.5671	-112.509	-1.94108	53.80337	15.10728	-115.863	-54.7844	-62.2291	-133.128
2004	12.76129	-83.7046	-121.956	5.2712	68.84669	5.23048	-125.218	-50.9977	-61.727	-139.237
2005	18.72885	-96.6495	-137.72	9.84081	80.59653	29.8751	-140.11	-53.5778	-65.5709	-153.633
2006	29.57596	-100.089	-143.921	20.04702	101.3687	43.63734	-146.995	-53.1595	-66.8956	-169.828
2007	24.80139	-109.691	-154.048	29.31235	118.8986	55.80171	-162.095	-53.8175	-70.2456	-192.051
2008	26.48737	-108.266	-159.603	35.98459	137.6718	67.16677	-172.446	-55.6671	-73.7387	-220.789

Table for Annual variation of Z_q for all stations

Year	Alibag	Guam	San juan	Belsk	CLF	Wingst	Boulder	Abisko	Sodankyla	Barrow
1985	-480.324	-342.298	1744.108	-329.541	-252.934	-306.179	892.1821	-225.133	-235.33	-61.8202
1986	-430.524	-329.7	1599.662	-301.48	-233.173	-282.613	828.3019	-218.837	-227.378	-84.6854
1987	-411.597	-321.225	1447.582	-278.937	-217.062	-262.343	752.2391	-214.782	-223.146	-106.757
1988	-402.285	-320.124	1309.999	-247.279	-190.874	-232.46	689.9854	-199.395	-206.955	-111.55
1989	-390.357	-303.305	1170.147	-211.34	-160.732	-198.573	632.5609	-175.53	-185.057	-104.432
1990	-386.791	-289.614	1023.031	-189.406	-142.331	-177.56	566.0689	-173.618	-180.591	-120.184
1991	-287.7	-265.309	875.6335	-165.31	-121.562	-153.583	508.6563	-158.06	-165.707	-121.624
1992	-285.082	-223.695	721.7635	-148.025	-109.52	-138.38	442.1551	-155.597	-162.394	-128.193
1993	-271.54	-166.134	561.1007	-127.894	-95.9463	-119.674	372.1331	-142.88	-151.033	-123.763
1994	-239.346	-104.322	402.7362	-99.9571	-76.3363	-94.1142	301.3297	-123.444	-129.248	-123.073
1995	-200.422	-55.4402	242.4215	-75.4753	-60.6955	-73.3135	217.8386	-104.747	-108.416	-123.787
1996	-141.368	-3.01766	85.23647	-49.2828	-44.9855	-51.3952	129.8062	-84.8247	-86.1242	-120.416
1997	-78.6827	50.8165	-74.4872	-14.5058	-21.2111	-19.8547	40.7692	-54.057	-54.3224	-101.963
1998	-14.1376	109.4989	-230.784	25.31332	11.83207	18.58992	-45.7618	-13.809	-12.2268	-66.4644
1999	36.36081	160.024	-392.402	58.97976	38.99124	51.91848	-147.368	23.35801	26.32726	-28.6666
2000	93.15244	196.7321	-545.886	94.85134	71.27396	90.21537	-250.291	64.73726	68.74886	11.36933
2001	160.085	219.1398	-699.354	132.2221	99.09807	123.5802	-361.649	104.096	109.8429	50.83266
2002	232.1877	240.9416	-853.878	170.7022	129.5824	159.7981	-471.484	150.2236	157.1354	96.59205
2003	352.0321	253.5072	-995.509	216.9642	169.5843	204.8546	-568.753	202.1763	208.6755	154.9376
2004	446.1682	266.4908	-1153.78	249.0278	195.6673	235.628	-680.054	235.3503	244.6261	185.1584
2005	537.2682	281.96	-1311.77	283.0413	223.7161	269.1229	-789.264	270.3806	280.9016	218.4665
2006	622.4503	297.9224	-1476.59	305.801	241.6125	291.2213	-910.123	298.7046	309.6234	236.4888
2007	713.8999	315.0633	-1637.93	335.8458	262.9624	319.2262	-1018.83	332.4922	344.372	270.6235
2008	826.6681	332.0761	-1811.08	365.6941	283.1494	345.8946	-1130.49	363.2728	377.7013	302.9936